# 9th Quarterly Progress Report to the FEDERAL HIGHWAY ADMINISTRATION (FHWA)

## On the Project: THE IMPACT OF WIDE-BASE TIRES ON PAVEMENT DAMAGE DTFH61-11-C-00025

**For period**
**April 1st to June 30th 2013**

**Submitted by**
**Illinois Center for Transportation**
**University of Illinois at Urbana-Champaign**

| FHWA Project | DTFH61-11-C-00025 | FY: 2013 | Quarter: 9 | April - June |
|---|---|---|---|---|
| Research Agent | Illinois Center for Transportation | | | |
| Principal Investigator | Imad L. Al-Qadi | | | |

| PHASE | RESEARCH TASK | 2011 | | | | | | | | | 2012 | | | | | | | | | | | | 2013 | | | | | | | | | | | | ESTIMATED % COMPLETION |
|---|---|---|---|---|---|---|---|---|---|---|---|---|---|---|---|---|---|---|---|---|---|---|---|---|---|---|---|---|---|---|---|---|---|---|---|
| | | A | M | J | J | A | S | O | N | D | J | F | M | A | M | J | J | A | S | O | N | D | J | F | M | A | M | J | J | A | S | O | N | D | |
| 1 | 1.1. Comprehensive literature review and synthesis on past and current research | 20 | 60 | 90 | 100 | | | | | | | | | | | | | | | | | | | | | | | | | | | | | | 100 |
| | 1.2. Experimental plan and modeling framew ork | | | 50 | 60 | 80 | 100 | | | | | | | | | | | | | | | | | | | | | | | | | | | | 100 |
| | 1.3. Implementation and marketing plan | | 10 | 50 | 70 | 80 | 100 | | | | | | | | | | | | | | | | | | | | | | | | | | | | 100 |
| | 1.4. Phase I report | | | 60 | 70 | 80 | 100 | | | | | | | | | | | | | | | | | | | | | | | | | | | | 100 |
| | 1.5. Conference call w ith panel | 0 | 50 | | | 100 | | | | | | | | | | | | | | | | | | | | | | | | | | | | | 100 |
| | 1.6. Presentations to relevant conferences and symposiums | | | | | | | | | | | | | | | | | | | | | | | | | | | | | | | | | | 0 |
| 2 | 2.1. Prepare experimental equipment, test structures, and instrumentation | | | | | 0 | 0 | 0 | 0 | 0 | 10 | 30 | 40 | 45 | 50 | 60 | 70 | 85 | 90 | 95 | 100 | | | | | | | | | | | | | | 100 |
| | 2.2. Conduct experiments, including material characterization and accelerated loading | | | | | | 0 | 0 | 0 | 0 | 5 | 10 | 20 | 25 | 30 | 40 | 50 | 60 | 70 | 40 | 40 | 40 | 45 | 50 | 55 | 55 | 57 | 60 | | | | | | | 60 |
| | 2.3. Conduct modeling | | | | | 0 | 0 | 0 | 0 | 0 | 1 | 2 | 5 | 6 | 8 | 10 | 20 | 25 | 30 | 30 | 35 | 35 | 40 | 45 | 50 | 50 | 53 | 55 | | | | | | | 55 |
| | 2.4. Development of analysis tool | | | | | | | | | | | | | 0 | 0 | 0 | 0 | 5 | 5 | 10 | 15 | 15 | 20 | 25 | 35 | 40 | 42 | 45 | | | | | | | 45 |
| | 2.5. Delivery of draft Phase II report and analysis tool | | | | | | | | | | | | | | | | | | | | | | | | | | | | | | | | | | 0 |
| | 2.6. Present to relevant conferences and sumposiums | | | | | | | | | | | | | | | | | | | | | | | | | | | | | | | | | | 0 |
| | 2.7. Prepare article and technical papers | | | | | | | | | | | | | | | | | | | | | | | | | | | | | | | | | | 0 |
| | Estimated Progress (%) | 1 | 3 | 7 | 8 | 10 | 11 | 11 | 11 | 11 | 13 | 15 | 19 | 21 | 23 | 27 | 33 | 38 | 43 | 41 | 40 | 38 | 42 | 45 | 49 | 50 | 51 | 53 | | | | | | | 53 |
| | Planned Progress (%) | 1 | 3 | 7 | 10 | 13 | 17 | 21 | 25 | 29 | 33 | 36 | 40 | 44 | 47 | 51 | 55 | 59 | 61 | 63 | 64 | 66 | 68 | 70 | 71 | 73 | 75 | 77 | 81 | 85 | 89 | 93 | 97 | 100 | 66 |

**QUARTERLY PROGRESS REPORT**

**QUARTER 9**

**The Impact of Wide-Base Tires on Pavement Damage – A National Study**

## 1. Work performed

During this quarter, the following tasks have been accomplished:

- Annual technical advisory committee meeting was conducted at McLean, Virginia on May 30th 2013. The attendees included representatives from Michelin, Rubber Manufacture Association, state DOTs (Texas, Minnesota, Virginia, Florida, Montana, Oklahoma, and Illinois), University of Illinois, Delft University, University of California, Davis, and FHWA. Full details of the meeting agenda and presentations can be found in the meeting minutes (Appendix C).
- Multiple FEM run and analysis were completed for the thin and thick pavement cases. The cases comprised of varying layer material properties and loading combinations. The corresponding summary of results was presented at the technical committee meeting. Further details of the completed FEM simulations are indicated in Appendix B.
- Experimental data gathered from the Council for Scientific and Industrial Research (CSIR) at South Africa was used to justify the importance of considering three-dimensional contact stresses in pavement design. Sets of equations were established to determine the vertical and transverse contact loads. Input parameters include the tire type, applied load, tire inflation pressure, distance along the contact length, and two regression parameters.
- Contact stress data from CSIR were organized for the Artificial Neural Network (ANN) modeling
- Testing at Florida and UC Davis were fully completed. Cores from Florida for material characterization were sent to the Advanced Transportation Research Engineering Laboratory. Moreover, shipping materials was sent to UC Davis for safe transport of the samples cores requested by the Illinois Center for Transportation.
- US23 truck testing at Ohio was completed, including the two mainline and ramp sections.
- The data from the three locations (Florida, UC Davis and Ohio) were organized and have been incorporated into the data management interface.

2. **Work to be accomplished next quarter**

- Material characterization of the test sections at Florida and UC-Davis will be initiated. Reports from both locations on construction and instrumentation will be provided.
- US23 test sections will be handed back to the contractor for resurfacing per ODOT. The data will then be uploaded electronically for access by the research team.
- Analysis of the pavement response data collected from Florida, UC-Davis, and Ohio will continue. More details on the ANN can be found in Appendix A.
- Mesh sensitivity analysis of the tire-inflated model will be performed.
- FEM analysis of pavement structures will continue.

3. **Problems encountered**

- Contact stresses were deemed to be inaccurate due to the width assumption. CSIR defines the influence area under the premise that the tire is smooth and in full contact with the pin. The input file generation Python scripts mesh were altered to generate a new tire imprint mesh suitable for nodal forces. Remembering that the previous mesh configuration accounted for contact stresses (pressure applied over a given area), whereas the new tire imprint considers nodal forces – simulating how the instrumented pins indirectly measured the contact loads.

.

4. **Current and cumulative expenditures**

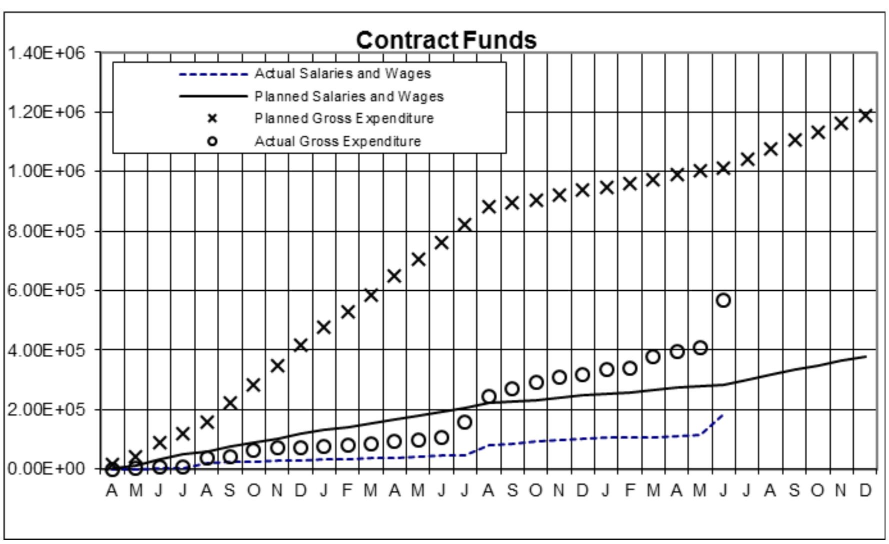

## 5. Planned, actual, and cumulative percent of effort

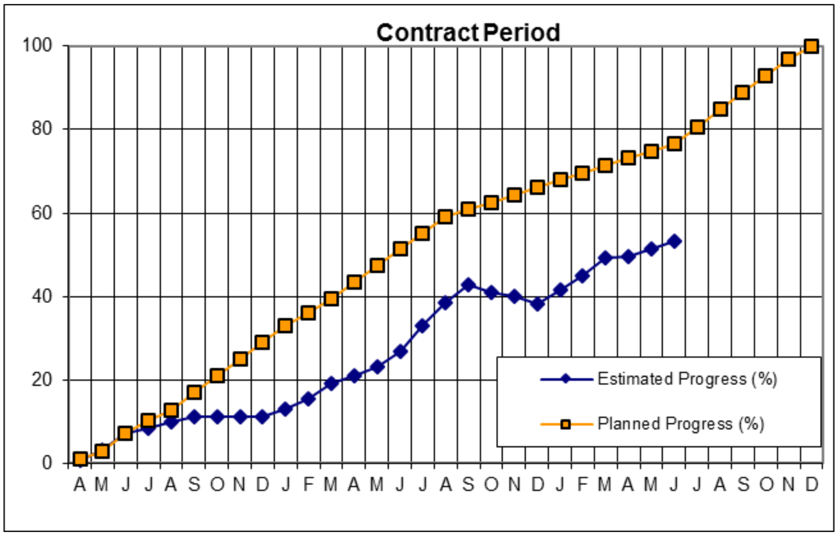

# APPENDIX A

## DATABASE MANAGEMENT

As mentioned in the previous quarter report, a framework has been developed to organize the pavement response data. Data provided from the test sections were filtered and organized in the main database. A user-friendly interface was developed to allow easy access to the "organized" database that contains all the existing and new data sources. New data from Florida DOT, Ohio SPS-8 were organized and included in the main database.

All the new data (as of June 2013) provided by Florida DOT, Ohio SPS-8 and UC Davis, were organized and included in the interface. The content of data provided by Florida and Ohio were described in the previous report. The test run in the UC-Davis included 5-in high RAP surface layer and 2-in AC wearing surface layer. Instrumentation included strain gauges in both longitudinal and transverse directions under the AC and RAP base layers. Pressure cells were installed under the aggregate base layer. Also, the Multi-Depth Deflectometer (MDD) was installed in the layers, which measured the deflection of different points within the depth of the pavement layers rather than a specific point. Figure 1 and 2 how the updated interface environment for Florida DOT and UC-Davis databases, respectively.

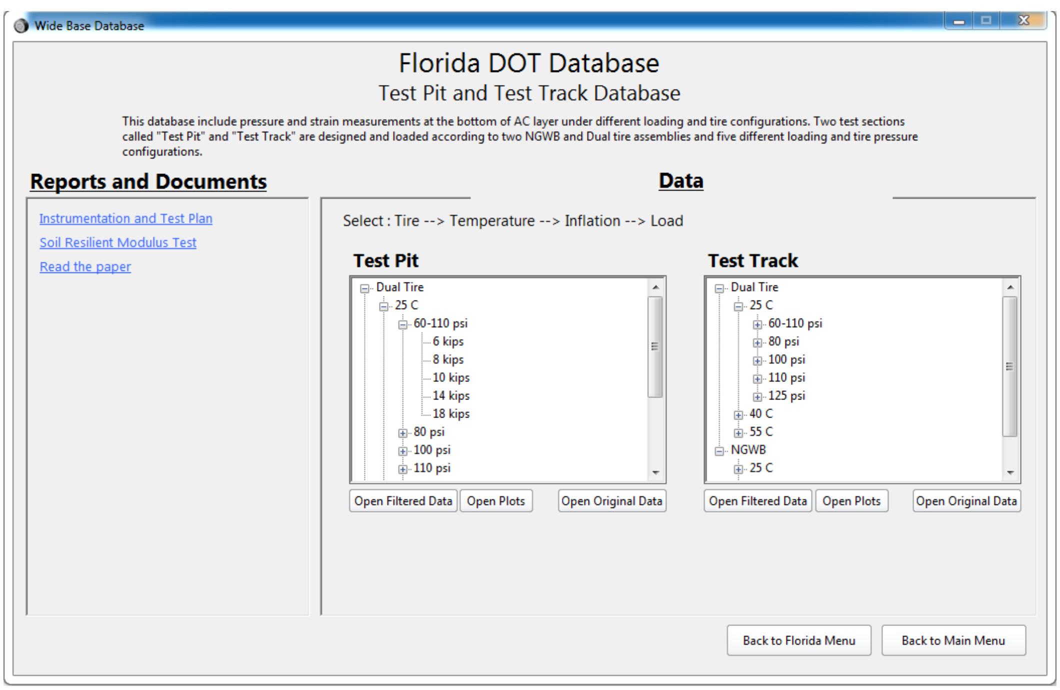


**Figure 1. Florida DOT test pit and test track database**

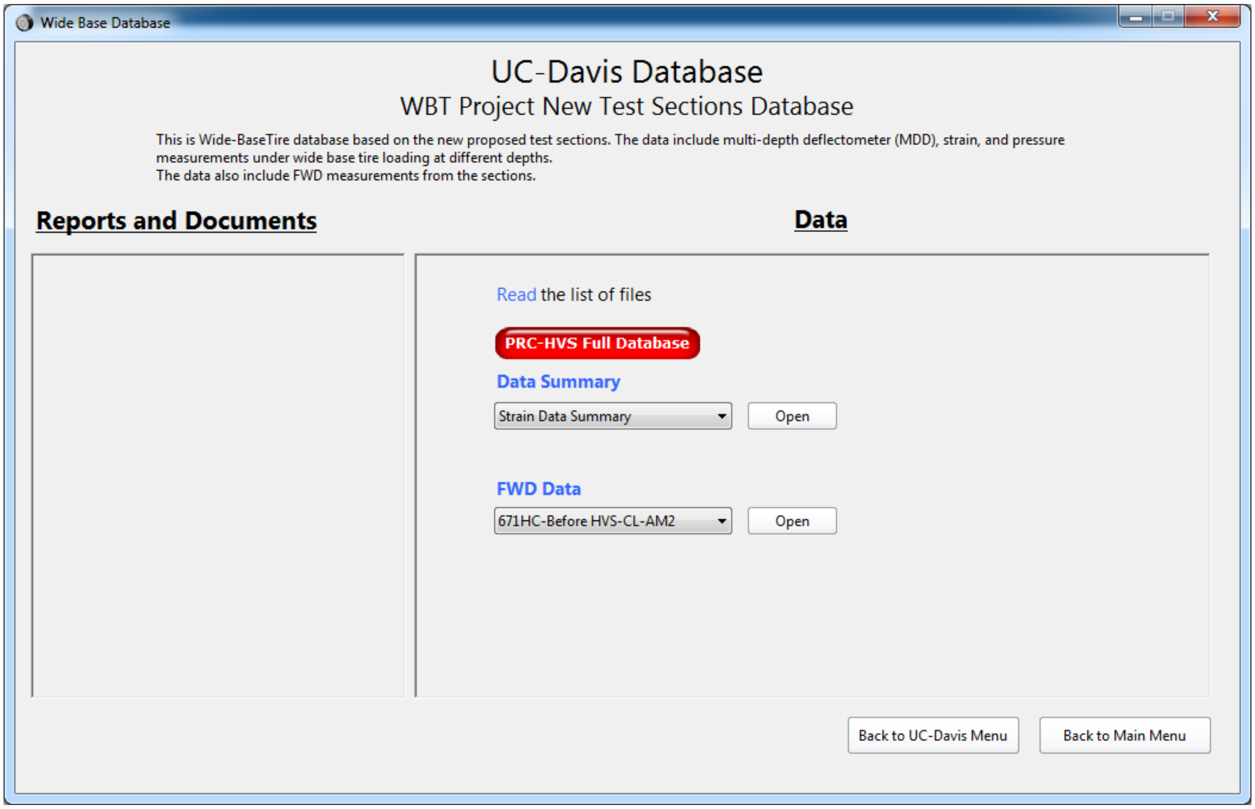


**Figure 2. UC-Davis new test sections database**

### Tire Contact Stress Analysis – Artificial Neural Networks Approach

In this section the tire contact stress data provided by South Africa, will be analyzed. The data included two tire types traversing over 42 instrumented pins, which measured the contact force induced by the tire. Different loading and tire inflation pressure combinations were used in this test. The tire footprint pattern and the resulting contact forces (and stresses) are incremental input for the finite element modeling of tire-pavement interface.

To allow developing tire contact stresses predictive models, artificial neural networks (ANN) will be utilized. ANN is one of the soft computing techniques, which is heavily robust and accurate in modeling uncertain data with many explicit or implicit explanatory variables. A two-step process will be taken in analyzing the data. Assuming a constant speed for all runs, the first step includes tire footprint pattern prediction according to the tire type (dual vs. wide-base), loading and tire inflation pressure. The predicted output of the first step is the number of actuated pins (in x direction), and the length of reading by each pin (in y direction) while the tire is traversing over the instrumented pins. Combination of this x and y axes will be a good representative of the tire footprint according to the pin assembly. In the second step, based on the predicted footprint and various loading and tire inflation pressure combinations, the forces under each pin will be predicted. The resulting predicted forces will be compared to the actual readings from the pins to verify the accuracy of the model. The outcome can be presented as 3D forces or 3D contact stresses

# APPENDIX B

## FINITE ELEMENT MODELING

Multiple number of FEM thin and thick pavement cases were completed. Table 1 indicates the status of the thin pavement cases, wherein the green highlighted cell symbolizes full analysis completion. The first column from the left indicates the pavement structure under analysis and the loading cases are listed from L1 to L12.

**Table 1. Status of thin pavement FEM cases**

| Thin | LOAD CASE | | | | | | | | | | | |
|---|---|---|---|---|---|---|---|---|---|---|---|---|
| | WBT | | | | | DTA | | | | | | |
| | L1 | L2 | L3 | L4 | L11 | L5 | L6 | L7 | L8 | L9 | L10 | L12 |
| AC75W_B150W_SGW | | | | | | | | | | | | |
| AC75W_B150W_SGS | | | | | | | | | | | | |
| AC75W_B150S_SGW | | | | | | | | | | | | |
| AC75W_B150S_SGS | | | | | | | | | | | | |
| AC75S_B150W_SGW | | | | | | | | | | | | |
| AC75S_B150W_SGS | | | | | | | | | | | | |
| AC75S_B150S_SGW | | | | | | | | | | | | |
| AC75S_B150S_SGS | | | | | | | | | | | | |
| AC125W_B150W_SGW | | | | | | | | | | | | |
| AC125W_B150W_SGS | | | | | | | | | | | | |
| AC125W_B150S_SGW | | | | | | | | | | | | |
| AC125W_B150S_SGS | | | | | | | | | | | | |
| AC125S_B150W_SGW | | | | | | | | | | | | |
| AC125S_B150W_SGS | | | | | | | | | | | | |
| AC125S_B150S_SGW | | | | | | | | | | | | |
| AC125S_B150S_SGS | | | | | | | | | | | | |
| AC125W_B600W_SGW | | | | | | | | | | | | |
| AC125W_B600W_SGS | | | | | | | | | | | | |
| AC125W_B600S_SGW | | | | | | | | | | | | |
| AC125W_B600S_SGS | | | | | | | | | | | | |
| AC125S_B600W_SGW | | | | | | | | | | | | |
| AC125S_B600W_SGS | | | | | | | | | | | | |
| AC125S_B600S_SGW | | | | | | | | | | | | |
| AC125S_B600S_SGS | | | | | | | | | | | | |

Nomenclature of the cases is simplified to “AC75W_B150W_SGS,” as an example.

Where AC = asphalt concrete layer,

75W = asphalt concrete layer thickness of 75mm, with a “WEAK” material property,

B = base (granular) layer,

150W = base layer thickness of 150 mm, with a “WEAK” material property, and

SGW = subgrade layer with indefinite thickness and “STRONG” material property.

The following table indicates the status of the thick pavement FEM cases, with similar definitions as the thin pavement FEM cases.

**Table 2. Status of thick pavement FEM cases**

| Thick | LOAD CASE | | | | | | | | | | | |
|---|---|---|---|---|---|---|---|---|---|---|---|---|
| | WBT | | | | | DTA | | | | | | |
| | L1 | L2 | L3 | L4 | L11 | L5 | L6 | L7 | L8 | L9 | L10 | L12 |
| AC125W_B150W | | | | | | | | | | | | |
| AC125W_B150S | | | | | | | | | | | | |
| AC125S_B150W | | | | | | | | | | | | |
| AC125S_B150S | | | | | | | | | | | | |
| AC125W_B600W | | | | | | | | | | | | |
| AC125W_B600S | | | | | | | | | | | | |
| AC125S_B600W | | | | | | | | | | | | |
| AC125S_B600S | | | | | | | | | | | | |
| AC412W_B150W | | | | | | | | | | | | |
| AC412W_B150S | | | | | | | | | | | | |
| AC412S_B150W | | | | | | | | | | | | |
| AC412S_B150S | | | | | | | | | | | | |
| AC412W_B600W | | | | | | | | | | | | |
| AC412W_B600S | | | | | | | | | | | | |
| AC412S_B600W | | | | | | | | | | | | |
| AC412S_B600S | | | | | | | | | | | | |

As aforementioned, the summary of results were presented at the annual technical committee advisory meeting at McLean, Virginia last May 30, 2013. However, the team determined that the contact stresses do not simulate realistic 3D tire loading. The inaccuracy is due to the assumed influence width of 17mm. As the tires traverse over the instrumented pins, the measuring device assumes that the tire is smooth and in full contact with the pin. However, due to the complex nature of the tire ribs, these assumptions are deemed to be invalid. As shown in Figure 3, pin-tire contact varies, thereby violating the assumed uniform influence width.

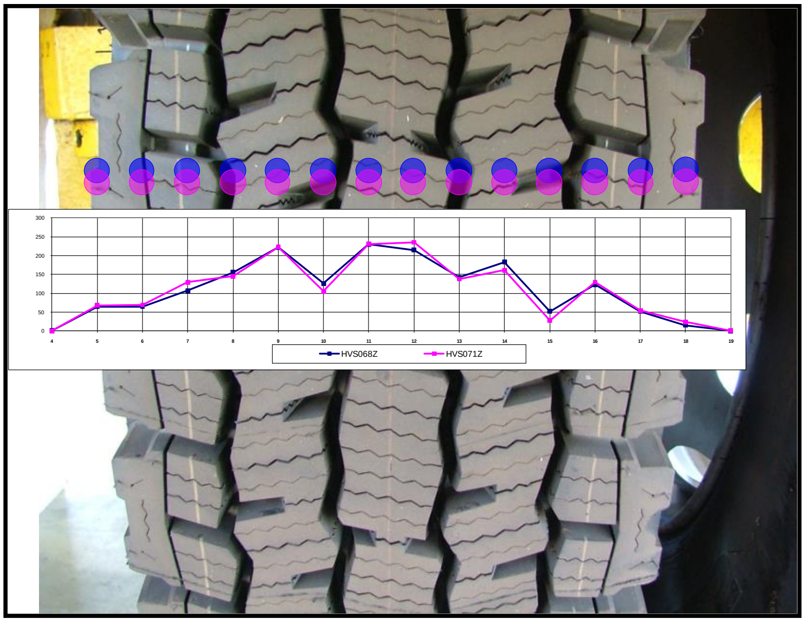


**Figure 3. Sample approximate lateral position of the tire over the instrumented pins.**

The modeling team determined that the static imprints cannot generate the accurate contact area to calculate the stresses. Therefore, instead of applying a variation of pressure over a given discretized contact area, the tire imprint of the model was altered to simulate the SIM pad assembly. The excitation was then defined as nodal forces, which can be directly calculated from the data provided by CSIR, and FEM simulations has initialized from this newly defined loading imprint.

## APPENDIX C

## ANNUAL TECHNICAL ADVISORY COMMITTEE MEETING MINUTES

### TPF-5(197) The Impact of Wide-Base Tires on Pavement Damage - A National Study
### Technical Advisory Committee Phase II Meeting
### TFHRC, McLean, VA
### May 30, 2013

### Attendance

A meeting of the FHWA National study for "The Impact of Wide-Base Tires on Pavement Damage" was held at FHWA Turner-Fairbanks Highway Research Center, on May 30, 2013. Those present for the meeting were:

Stan Lew (Michelin)
Joel Neff (Michelin)
Van Teeple (Michelin)
Keith Brewer (Rubber Manufacturer Association)
Steve Butcher (Rubber Manufacturer Association)
Larry Buttler (Texas DOT)
Shongtao Dai (Minnesota DOT)
Brian Diefenderfer (Virginia DOT)
James Green (Florida DOT)
Dan Hill (Montana DOT)
Terri Holley (Oklahoma DOT)
David Lippert (Illinois DOT)
Imad Al-Qadi (University of Illinois)
Aaron Coenen (University of Illinois)
Jaime Hernandez (University of Illinois)
Angeli Gamez (University of Illinois)
Mojtaba Ziyadi (University of Illinois)
Tom Scarpas (Delft University)
Rongzong Wu (UC Davis)
Eric Weaver (FHWA-TFHRC)

## Introduction

Eric Weaver gave an overview of the meeting logistics and opened the meeting with self-introductions. Imad Al-Qadi then started the presentation with a brief overview of the project and presentation topics.

## Presentation and Panel Discussions

### *Tire Contact Stress*

Jaime Hernandez discussed the three-dimensional (3D) contact stress data acquired from the Council of Scientific and Industrial Research (CSIR) in South Africa. The experimental program consisted of various combinations of tire inflation pressure (552 to 862 kPa) and tire loading (26 to 80 kN) for the two tires considered in the research study: WBT 455/50 R22.5 and DTA 275/80 R22.5. In addition, a DTA with differential tire inflation pressure was also included in the test matrix. The stress-in-motion system (SIM) at CSIR was introduced, wherein a select number of steel pins measured the applied forces as the tires traversed the pad assemblies. A detail of the measuring pin was also illustrated. Tire imprints were also obtained for the contact area.

Keith Brewer commented on the conditioning of the tire surface prior to measuring the contact stresses and Eric Weaver suggested a follow up with Morris De Beer to determine if any tire conditioning process was performed.

Jaime Hernandez continued to explain the use of the load deflection curves that would be used to calibrate the finite element modeling (FEM) of the tire and the selection of the three out of ten optimum contact stress repetitions. The three optimum repetitions were selected by comparing the applied load by the HVS to the resultant force from the measurements. The presentation then proceeded to data processing, which included filtering of the measured forces using the developed Matlab script and calculation of the contact area based on the tire imprints using AutoCAD. In addition, a Python script was developed to provide summary plots of the 3D contact stresses and tire imprint geometry. Preliminary analysis was also discussed, including the effect of the tire type, range of inflation pressures and two extreme tire loading cases (26 and 80 kN) on the 3D contact stresses and contact areas.

### *Pavement Modeling*

Tom Scarpas introduced the thick pavement model development done by Delft University in cooperation with the University of Nottingham. The thick pavement structure was defined in order to initiate the mesh sensitivity analysis. The mesh size was reduced in the depth direction to provide a balance of accuracy and minimized computational time. In addition, along the tire imprint, a fine mesh was introduced in the transverse direction based on previous research at the University of Illinois. The sinusoidal contact stress distribution considered in FEM was also illustrated. Several inputs from the Smart Road data for the FEM included the 3D contact stresses and tire footprint dimensions of both the WBT and DTA, and layer material characteristics. Using the thick pavement case presented, a comparison of results using CAPA-3D by Delft University and Abaqus by University of Illinois will be performed. It was also emphasized that the surface layer needs to be realistically represented with viscoelastic properties. The analysis positions included the locations of the maximum tensile strains of the asphalt concrete at the top and bottom surfaces, maximum vertical compressive strain at the top of the subgrade, and maximum shearing strain in the asphalt layers. These responses will be considered as performance indicators and will be used in the design guides. Preliminary outputs of the analyses due to the effect of WBT and DTA loading patterns were presented.

Imad Al-Qadi commented on the location of the measurements when comparing the DTA and WBT and the importance of considering the tire wander in the analysis. In accordance to the maximum responses, Van Teeple added that the location of the maximum responses may occur in the lateral or longitudinal direction.

Tom Scarpas commented on the contact problem between the tire and pavement surface. Moreover, Eric Weaver remarked on the result comparison using CAPA-3D and Abaqus to ensure model agreement. Tom Scarpas mentioned that the comparison would be initiated with a linear elastic analysis for an easier adjustment and development of the FEM software.

Angeli Gamez introduced the FEM development performed at the University of Illinois. Using Abaqus, a dynamic-implicit analysis is considered to represent the effect of mass inertia and damping forces on the pavement responses. Similar to the cases presented by Delft University, linear viscoelastic material properties were used for the asphalt concrete layers and non-uniform 3D contact stresses were simulated. However, in terms of the granular materials, the thin pavement cases assumed non-linear stress-dependent properties, whereas the thick pavement cases considered elastic properties. A continuous moving load was also introduced in order to simulate the rolling pattern of the tire as it traverses over the pavement structure. Other finite element model parameters discussed included the use of infinite boundary elements and various layer interactions – all alluding to a more realistic representation of the pavement analysis.

The mesh sensitivity analysis was also discussed for both the thin and thick pavement structures to optimize the distribution and location of the finite elements which controls the computational time and accuracy of the model. BISAR was used for the comparison, with a 5% difference criteria defined. Results of the comparison showed a good agreement between the responses from BISAR and Abaqus which ensures that the mesh configuration was accurately represented.

Additionally, the FEM analysis matrix was introduced. The parameters included the pavement geometry, material property and loading cases (with various combination of inflation pressure and load for WBT and DTA).

Eric Weaver commented regarding the tire model. Imad Al-Qadi mentioned that tire material properties were obtained, however modeling of the tire is beyond the scope of the research study, which should be considered in future work. Van Teeple mentioned that the contact stresses being measured to compare the WBT and DTA is one of the many important variables. However, several factors, such as tire life, design details, and operating conditions, should also be considered and are closely related to the load deflection curves. Tom Scarpas suggested that if the tire models are calibrated at low speeds, then increasing the speeds can be implemented. And that the influencing factors of the tire imprint are important. Stan Lew emphasized that it is important to keep in mind that there are many factors that changes the responses and cannot generalize. Imad Al-Qadi suggested that the outcome of the research study should be considered in a way that it should be geared to be multi-faceted and account for new tire models apart from the scope of the research. Eric Weaver mentioned that the difficulty arise from obtaining an accurate tire model is the proprietary conditions and that feasibility of considering all tire types and testing.

Jaime Hernandez presented the use of the Abaqus Python Development Environment (PDE) to automate repetitive tasks on the input file generation. PDE enables the user to perform parametric studies, create and modify models, and access the output database in an efficient manner. In accordance to the FEM inputs, the 3D contact stress measurements from CSIR were transcribed onto the discretized loading imprint.

Imad Al-Qadi commented that a South Dakota study observed the difference in truck mileage impact on low and high volume roads and its importance on pavement damage and corresponding cost.

The asphalt concrete material properties were obtained from the LTPP Data Release # 26, in order to represent two extreme materials (weak and strong). The selection was performed using a statistical analysis with an NMAS criterion for each asphalt concrete layer (wearing surface, intermediate layer and base layer). In addition, the thin pavement cases considered the cross-anisotropic stress-dependent material property for the granular base layer. Similar to the AC layer, the weak and strong (extreme) material properties were generated. Another important FEM parameter was the temperature distribution in the asphalt concrete layer. Based on a past research study, the temperature distributions for various asphalt concrete thickness combinations was determined. Imad Al-Qadi commented that due to the viscoelastic property of the asphalt concrete, it becomes dependent on speed of the load and the temperature. However, the granular materials are not considered to be temperature dependent.

Using the discussed input parameters, preliminary FEM runs were performed for both the thin and thick pavement cases due to the effect of the load and material property combinations. A sample of the output was also presented.

Van Teeple commented on the discontinuity of strain indicates no bonding between the layers. Jaime Hernandez mentioned that the FEM simulates field conditions wherein the asphalt concrete is not fully bonded to the granular material. Imad Al-Qadi emphasized that shearing has a major effect on distresses and should be considered. Eric Weaver mentioned that the damage models are calibrated based on test data; however, as the FEM and field results capture all directions, this could lead to the development of new damage models.

***Data Management***

Mojtaba Ziyadi presented the process of data management, filtering process and its importance for the Artificial Neural Network (ANN). The field and accelerated pavement testing (APT) data would be used to train and test the ANN model. Main data sources that were used for the in-progress interface development include the test sections at the University of Illinois, Florida DOT, UC Davis, Ohio DOT, and Virginia Smart Road.

The data from Florida and Ohio is currently in the filtering stage using a Matlab script. The filtering process includes the transfer of data to origin, smoothing using the Robust Local Regression Method, and extraction of local extremes. Eric Weaver commented on the data extraction, which is a robust and labor intensive process in order to obtain the peak points for the responses. Mojtaba Ziyadi added that automating the filtering process is difficult, as the noise can be dependent on the various factors, e.g., sensor, and therefore, requires user effort in determining the appropriate filter. Imad Al-Qadi emphasized that proper grounding could also affect the data. Preliminary response data from Ohio and Florida were presented to illustrate filtering.

In order to organize all the data, a user-friendly interface was initiated. The interface consists of the response data, reports, instrumentation schematic and pictures for added documentation. The future plans of data management and organization includes the creation of ANN, which is a robust and nonlinear statistical learning technique. It trains from a given data and extracts the knowledge to interpolate cases within the provided boundary and accuracy of the data. Benefits of using ANN includes the ability to predict pavement damage caused by various loading and tire configurations with less computational time. The training stage of the ANN model will include the FEM results from the thin and thick pavements, while field and APT data will be used for the validation.

***Laboratory Testing***

Eric Weaver mentioned that one of the hindrances that prevent the penetration of the WBT is the hard sell of balancing fuel economy with offsetting the new cost of the retrofit. However, fleets and owners have seen the benefits of incorporating them, and they estimated 20% of the trucks have at least one axle equipped with WBT. Some issues that were discussed related to the difficulty to re-thread the tire, uneven tire wear, and inharmonious state limits regarding tire and axle limits, and axle-load configurations – which should all be acknowledged in the implementation plans.

Aaron Coenen presented the material acquisition and sample preparation performed at the Ohio test section in September 2012. Research engineers and graduate students from the Illinois Center for Transportation (ICT) created a “mobilized” lab setup at the asphalt plant in Ohio in order to acquire the appropriate amount of specimens for material characterization. An area adjacent to the satellite testing building of the plant housed the “mobilized” lab, which includes portable gyratory compactors, small ovens and various testing equipment. Alongside the interval collection of specimens, Illinois graduate students documented the paving sequence of all the layers of the test sections to ensure that the material at instrumented area is properly characterized.

The total number of collected specimens were divided between the University of Illinois and Texas A&M University. The remaining specimens are then divided into various laboratory tests, including dynamic modulus, semi-circular bending, indirect tension (IDT), disk-shaped compact, and push-pull. Specimen fabrication for each tests were illustrated and test specifications were briefly discussed, as performed at ICT. Another important factor was the influence of the target density, which should reflect the in-field density. By preparing the specimens at the same density as laid on the field test sections, not only would the FEM cases have a more accurate material property characterization; but also this method would monitor the consistency of the production truck-by-truck.

Adjustment for field cores from the Florida and UC Davis test sections was mentioned, as the thin pavements does not meet the required test specimen dimension of the dynamic modulus and push-pull tests. It was suggested to compensate the dynamic modulus data using the IDT creep compliance test, and use IDT fatigue for the push-pull test.

Brian Diefenderfer recommended to perform the dynamic modulus test on the IDT specimen. Imad Al-Qadi mentioned that the modulus is only reflected in two different directions, which may sacrifice the accuracy of the process. Jamie Green mentioned that they gathered a limited number of data using the IDT specimen for the dynamic modulus test. Eric Weaver commented that during a study at Connecticut, the same scenario was observed and there is a draft procedure prepared by Richard Kim. Imad Al-Qadi mentioned that the main goal of the material characterization was to obtain the Prony series for the viscoelastic property, which could be obtained via the creep compliance test.

Eric Weaver summarized the pre-construction meeting that was organized at Ohio regarding the refinement of instrumentation and construction details of the test sections. Testing was initiated in Ohio, however, it was performed towards the end of the 2012 under cold weather conditions. This then affected the magnitude of the responses. In addition, the contractor was not satisfied with the appearance of the surface layer and decided to set a reconstruction date in June for resurfacing (this process will also remove the instruments in place). The truck load test to be performed this summer was also mentioned.

***Instrumentation and Field Testing***

***Florida***

James Greene presented the instrumentation and testing phases of the test sections at Florida, and a brief overview of the Florida DOT APT facility. The facility includes eight test tracks, two test pits and a heavy vehicle simulator (HVS) with an independently controlled heating system. The cross sections of the test pit and test track sections were also discussed, along with the instrumentation schematic. The types of instruments for the test sections included 24 surface strain gauges (foil), 6 asphalt strain gauges (H-type), and 4 pressure cells. A preliminary filtered strain data was also presented. The construction, paving, and material sampling processes were also illustrated.

In terms of laboratory testing, both the granular and asphalt concrete materials were characterized. Asphalt concrete cores and loose mixture were also collected. Additionally, the HVS test matrix was defined and completed, and the response data was sent to the University of Illinois. Currently, shipment of the specimens is being arranged between the Florida DOT and the University of Illinois.

James Greene commented that the layer thicknesses are typical for Florida pavement designs consisting of a thin asphalt concrete layer and stiff base. Imad Al-Qadi mentioned that the HVS data from Florida would be used for FEM validation, considering the same material property and pavement geometry. It was also emphasized that by doing a collaboration with other agencies, such as the Florida DOT, it minimized the cost of paving a new test section and allowed access to various test sections with a limited budget.

Brian Diefenderfer referred to how the foil strain gauges were used in between layers and its constructability. Imad Al-Qadi commented that the foil gauges would be easily damaged. In Ohio, cores were removed and the foil gauges were placed on the circumference of the core at various depths. Florida, on the other hand, placed the foil strain gauges 3, 6 and 12 in away from the tire edge for surface data.

Imad Al-Qadi mentioned that the importance of considering a variety of test sections and material properties would provide a broad spectrum of analysis and affect the validation stage of the finite element models of the previously presented thin and thick pavements and ANN.

***UC Davis***

Rongzong Wu presented the instrumentation and testing phases of the test sections at UC Davis. The HVS response testing on two flexible pavements was recently completed and the life cycle assessment (LCA) framework was established. Similar to the case in Florida, the defined full depth recycling pavement structure was also connected to a Caltrans study.

The types of instrumentation included 8 strain gauges, 4 pressure cells, 1 multi-depth deflectometer (MDD) with three depths, and 12 thermocouples for the thick pavement section, whereas the thin pavement section included 6 strain gauges, 1 pressure cells, 1 multi-depth deflectometer (MDD) with four depths, and 12 thermocouples. A multi-depth deflectometer is constructed by stacking deflectometers on top of another to measure deflections at various depths. Unfortunately, few strain gauges malfunctioned during testing, which may be due to the construction process.

Tire imprints were also generated for both tires. More over the HVS testing program included a combination of pavement temperatures, various tire pressures and half axle load ranges, and lateral offsets. The testing sequence was initiated with the half axle loads below 18 kips to avoid possible damage. Each combination consisted of 100 repetitions with a constant speed of 8 kph and no wander. The thick section was tested between March 6$^{th}$ and April 15$^{th}$, with a total of 22,100 repetitions, whereas the thin section was tested between April 26$^{th}$ and March 20$^{th}$, with a total of 20,300 repetitions. Preliminary response data and surface rut contours were also presented.

In terms of the LCA, the selected scenarios were based on the traffic level and pavement structure. Additional analyses would also involve several factors including market penetration rates, tire types, traffic levels, and congestion levels. From the LCA, decision makers would gain an additional tool in considering the impact of WBT.

Van Teeple suggested a future discussion of the LCA, with regards to the needed tire-related inputs. Rongzong Wu commented that the life cycle inventory (LCI) is built from past studies of concrete and asphalt pavements, and from attendee inputs from an international workshop hosted by UC Davis. However, their LCI does not include tire materials. The lateral offset definition was clarified, wherein the zero offset was defined to be directly under the centerline of the tire.

Imad Al-Qadi mentioned that the location of the maximum responses varies, depending on the load applied and pavement thickness. Therefore, introducing the offset provides a more robust analysis of the pavement response.

Stan Lew commented that the WBT rim has a built-in 2 in outset, however the disk was modified because the American wheel does not fit with the hub. And checked if the 2 in outset was maintained and when mounted onto the hub the WBT would be out 2 in. Rongzong Wu mentioned that the centerline of the tires were checked and ensured that it lied on the predefined line of instruments. Eric Weaver emphasized that the meeting does not include firm conclusions but the fact that the effect of lateral offset it significantly important.

Van Teeple mentioned a paper from the University of Laval (2012) discussing the effect of the lateral offset and would be shared with the committee for better visualization.

A collective comment by the committee was focused on the location of the strain gauge in the middle of the DTA, instead of underneath one of the two tires to locate the maximum response when the tire is directly on top of the sensor (in comparison to WBT directly over the sensor). Imad Al-Qadi mentioned that there is available data for the WBT wander from the University of Illinois but none for DTA. One of the future plans would include a robust analysis of the current and future data. Therefore, conclusions cannot be drawn solely from the preliminary results.

***Ohio***

Angeli Gamez presented the instrumentation and testing phases of the test sections at Ohio. A brief description of the project purpose was discussed, by which the thick pavement structure consisted of various asphalt concrete thicknesses. In contrast to the Florida and Davis APT sections, Ohio used a controlled truck load test to compare the DTA and WBT with single and tandem axles.

The types of instruments consisted of linear variable differential transformer (LVDT), pressure cells, thermocouples, strain gauges and rosette strain gauges. The controlled truck loading test matrix was also presented. Replacement of instrumentations that malfunctioned occurred in late May and instrumentation was scheduled in June.

Imad Al-Qadi mentioned that Ohio may not complete the test matrix due to time constraint, and the matrix would be limited to regular loading scenarios with different speeds. In addition, the differential DTA case was requested to consider its significant impact, which was observed in the Smart Road project.

Eric Weaver commented on the complicated collaboration due to time constraint and instrumentation schematic change, as rosette strain gauges were not part of the initial plan of Ohio. Moreover, some part of the Legacy datasets, the lateral offset was varied cautiously to observe the variation. This data is available and could be useful for this research project.

In regards to the Ohio testing plan, a lateral offset was not part of the matrix. However, at higher speeds, involuntary lateral offsets would be apparent and cannot be easily controlled. Imad Al-Qadi added that though there is a time restriction and limitation on the test matrix, good data would be collected. Rongzong Wu commented that it is important to not only analyze the peak response but also the distribution, as wander in real traffic conditions varies highly. Van Teeple emphasized that lateral offset is highly critical and suggested that keeping track of the offset by mounting a camera onto the vehicle would track the lateral offset. Imad Al-Qadi assured that the lateral offset would be documented during the test runs. For each run, 20 passes would be completed. However, Eric Weaver clarified that pre-defined offsets were not set due to low repeatability.

***Future Plans***

Imad Al-Qadi concluded the presentation with the summary of future plans.

- Regarding the contact stresses, a detailed contact stress analysis of the DTA and WBT will be completed. Also, a future implementation of contact stress prediction would be done using FEM.
- In terms of pavement modeling, the matrix will be finished to provide a robust analysis considering the effect of the tire type, material property, loading characteristics and pavement structure.
- Material characterization in the laboratory will be completed for all the test sites.
- The field and APT collection and analyses will be finished and organized for all test sites. As data is received, it will be filtered and analyzed.
- Preliminary LCA scenarios will be established.
- Further marketing and future publications will be done.
    - There will be a WBT webinar regarding the contact stresses later this summer. Imad Al-Qadi added that there was a WBT webinar last fall.
- The data pool will be available in the future and will be easily accessible via ANN.

Eric Weaver commented that until all the data is sifted and the analysis is completed, conclusions cannot be drawn. Additionally, the committee need to think ahead regarding the technology transfer and most appropriate organization of the data and results (e.g. use of website interface). Imad Al-Qadi mentioned that the study has experienced some good delays, in terms of generating accurate pavement models, site construction and load testing. The committee is then encouraged to consider the low feasibility of completing and drawing strong conclusions on the project by December 2013. Eric Weaver stressed that the accuracy of the results weigh heavier than the planned project date completion.

After the technical discussion meeting, Eric Weaver commented on the application and implementation of the results into design guides. Additionally, the committee acknowledged the delays, however, the overall vision and expectations should be considered in a state DOT perspective. The research team is encouraged to consider and address the declined emphasis of the LCA aspect of the project. Alternative truck configuration should also be accounted and the committee members should participate in upcoming webinars to determine what other agencies, e.g. EPA, are considering. Moreover the value, implementation and practical use of the product is more important than the time it is received, the technical committee requests from the research team an answer regarding the time estimation for completing the project.

Imad Al-Qadi mentioned that the original proposal did not put a strong emphasis on LCA, but depending on the project budget, the technical panel may consider altering the proposal to allot for additional time for the LCA.

Eric Weaver thanked the attendees and closed the meeting at 4:30 p.m.

**Action Items:**

- Imad Al-Qadi will send out a brief presentation overview of the Artificial Neural Network and presentation copy to committee members.
- Preparations of tires before testing (De Beer)
- Send the paper on “Myth and Truth of Fatigue in Asphalt Concrete.”
- Imad Al-Qadi need to respond to the comments of the technical committee within a month of receiving them.

# APPENDIX D

# ANNUAL TECHNICAL ADVISORY COMMITTEE MEETING MINUTES

# Impact of Wide-Base Tires on Pavements – A National Study

5/30/2013





# Agenda

- 08:00-08:30 Introduction/Project Overview
- 08:30-09:15 Tire Contact Stress
- 09:15-10:00 Pavement Modeling (Delft/UIUC)
- 10:00-10:15 Break
- 10:15-11:00 Pavement Modeling (Thin & Thick)
- 11:00-12:00 Data Management
- 12:00-13:00 Lunch
- 13:00-13:45 Laboratory Testing
- 13:45-15:15 Instrumentation and Field Testing
- 15:15-15:30 Break
- 15:30-15:45 Future Plans Discussion
- 15:45-16:15 Technical Committee Discussion
- 16:15-16:45 Final Remarks
- 16:45 Adjourn



# Project Overview
# 8:10-8:30am

5/30/2013



# Project Overview

- Quantify the impact of WBT on pavement damage utilizing advanced theoretical modeling and validate results using full-scale testing
- Scope:
  - Contact stress measurements of tires (WBT & DTA)
  - APT of pavement sections
  - FEM modeling of pavement loading
  - Calculation of pavement damage



# Project Overview

- Phase I Tasks
  - 1.1. Comprehensive literature review and synthesis on past and current research
  - 1.2. Experimental plan and modeling framework
  - 1.3. Implementation and marketing plan
  - 1.4. Phase I report
  - 1.5. Conference call with panel
  - 1.6. Presentations to relevant conferences and symposiums
- Phase II Tasks
  - 2.1. Prepare experimental equipment, test structures, and instrumentation
  - 2.2. Conduct experiments (material characterization and APT)
  - 2.3. Conduct modeling
  - 2.4. Develop of analysis tool
  - 2.5. Delivery of draft Phase II report and analysis tool
  - 2.6. Present to relevant conferences and symposiums
  - 2.7. Prepare article and technical papers



# Project Overview

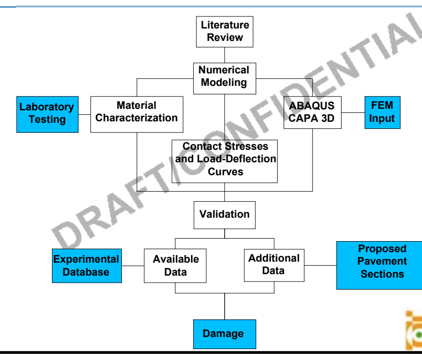

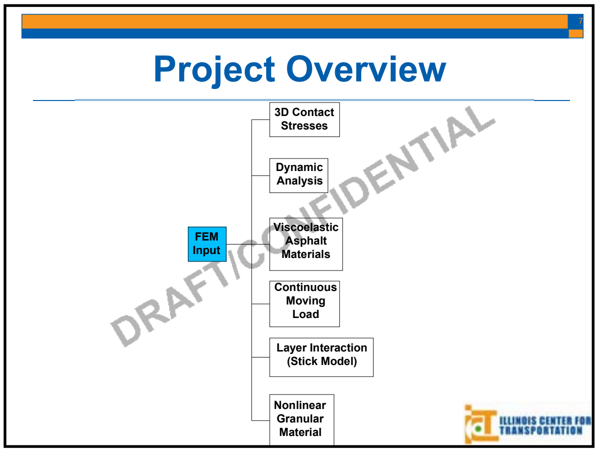
Project Overview
FEM Input
3D Contact Stresses
Dynamic Analysis
Viscoelastic Asphalt Materials
Continuous Moving Load
Layer Interaction (Stick Model)
Nonlinear Granular Material
DRAFT/CONFIDENTIAL
ILLINOIS CENTER FOR TRANSPORTATION

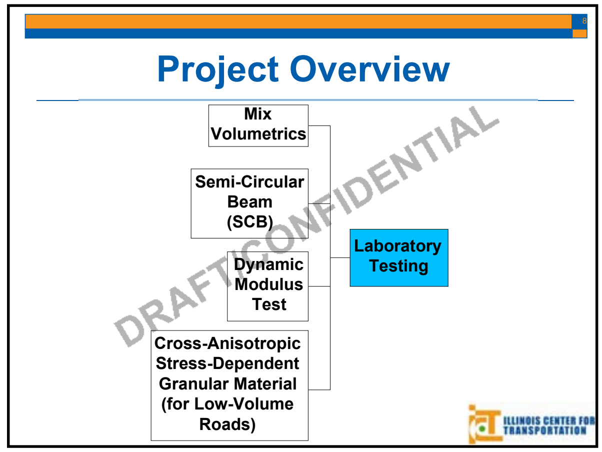
Project Overview
Mix Volumetrics
Semi-Circular Beam (SCB)
Dynamic Modulus Test
Cross-Anisotropic Stress-Dependent Granular Material (for Low-Volume Roads)
Laboratory Testing
DRAFT/CONFIDENTIAL
ILLINOIS CENTER FOR TRANSPORTATION

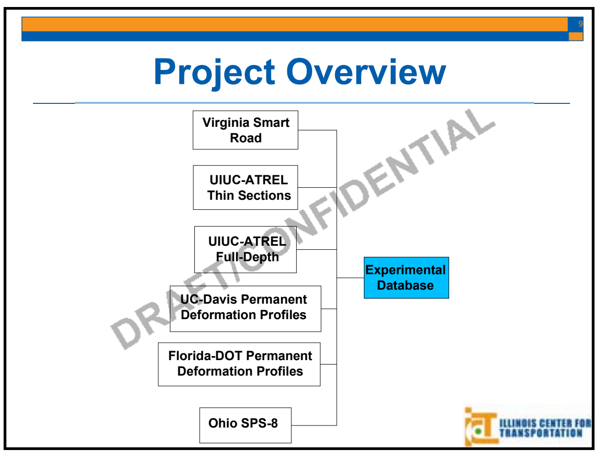
Project Overview
Virginia Smart Road
UIUC-ATREL Thin Sections
UIUC-ATREL Full-Depth
UC-Davis Permanent Deformation Profiles
Florida-DOT Permanent Deformation Profiles
Ohio SPS-8
Experimental Database
DRAFT/CONFIDENTIAL
ILLINOIS CENTER FOR TRANSPORTATION

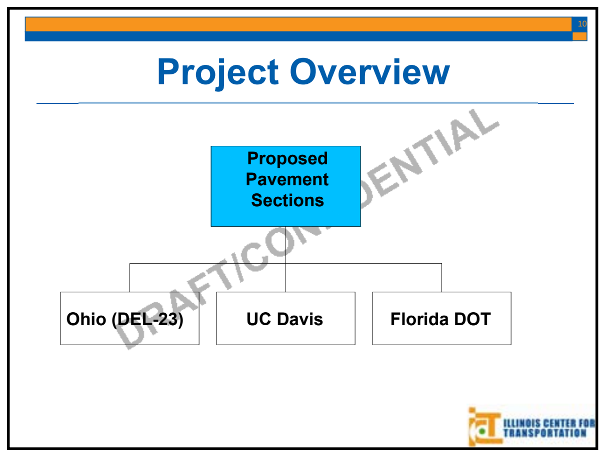
Project Overview
Proposed Pavement Sections
Ohio (DEL-23)
UC Davis
Florida DOT
DRAFT/CONFIDENTIAL
ILLINOIS CENTER FOR TRANSPORTATION

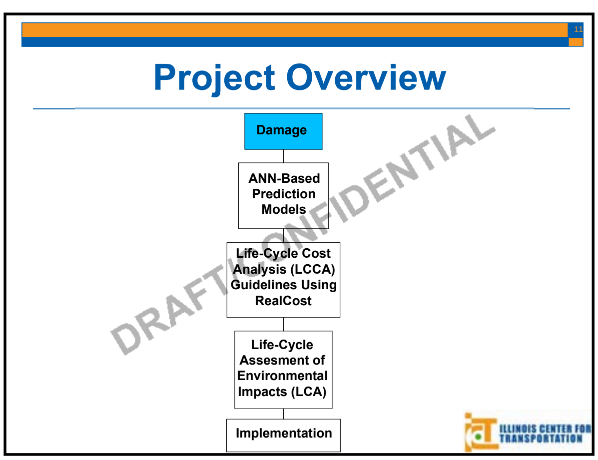
Project Overview
Damage
ANN-Based Prediction Models
Life-Cycle Cost Analysis (LCCA) Guidelines Using RealCost
Life-Cycle Assesment of Environmental Impacts (LCA)
Implementation
DRAFT/CONFIDENTIAL
ILLINOIS CENTER FOR TRANSPORTATION


COMMENTS!
DRAFT/CONFIDENTIAL
ILLINOIS CENTER FOR TRANSPORTATION

# Tire Contact Stress

**8:30-9:15am**

5/30/2013



## Outline

- Experimental Program
- Data Processing
- Contact Stress Distributions
- 3D Contact Stresses
- Tire Contact Area
- Maximum Rib Contact Length
- Summary



## Experimental Program

| Tire Type | Inflation Pressure (kPa) | Tire Loading (kN) | | | | |
|---|---|---|---|---|---|---|
| NGWB and Dual | 552 | 26.6 | 35.5 | 44.4 | 62.2 | 79.9 |
| NGWB and Dual | 690 | | | | | |
| NGWB and Dual | 758 | | | | | |
| NGWB and Dual | 862 | | | | | |
| Dual Only | 414/758* | | | | | |
| Dual Only | 552/758* | | | | | |

*Differential Tire Inflation Pressure

## Experimental Program: Tested Tires

WBT 455/50 R22.5

DTA 275/80 R22.5



## Experimental Program: Measuring System

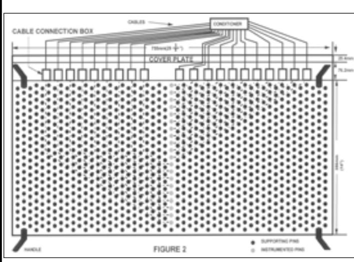

Single Pad Assembly
(SIM is composed by two Pads)

- Nominal Area: 840x417 mm
- 1020 Supporting Pins
  - 21 Instrumented Steel Pins



## Experimental Program

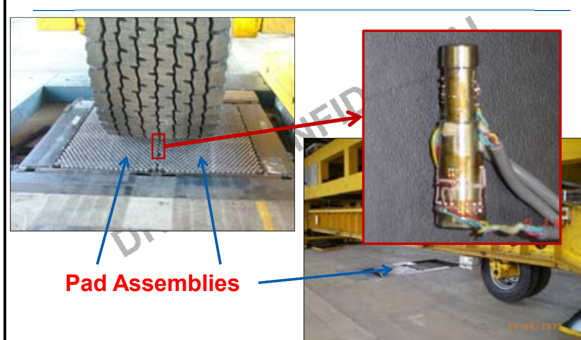

## Experimental Program

- **Lateral position of tires was fixed**
- **Pin measured applied force**
- **Average speed: 0.331m/s (1.19km/h)**
- **Sampling frequency: 1001hz**
- **Static imprints of tires obtained**
- **Load deflection curves were measured**
- **Each load combinations were repeated 10 times; optimum three repetitions were used**



## Pin Measurements in txt Format

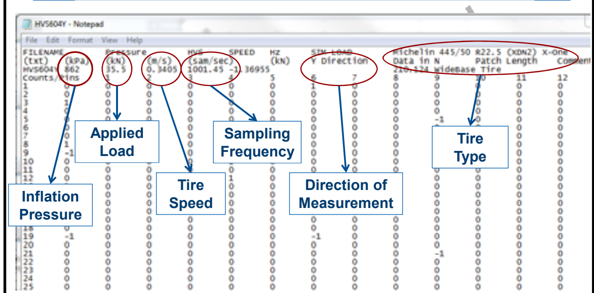


## Data Processing

- **Script written in Matlab:**
  - **Data filtered using moving average (window size = 20 measurements)**
  - **Simultaneous observation of three repetitions and filtered data**



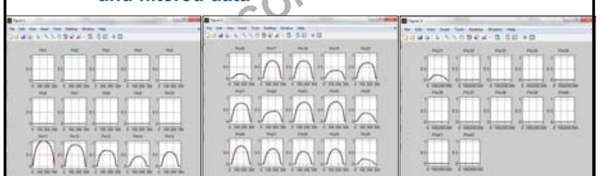

## Data Processing

- **Filtering data using moving average**

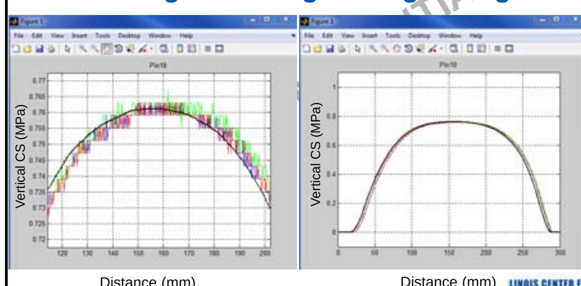


## Data Processing: Contact Area

- **Contact area from footprint (processed in AutoCAD)**
- **Contact length from pin measurements**



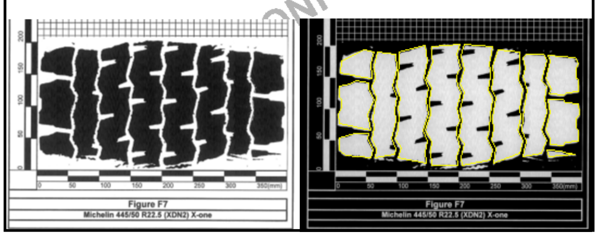


## Data Processing

- **Summary Plots (Python)**

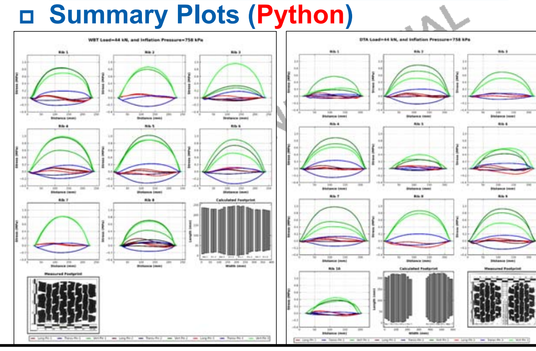

## Contact Stress Distributions

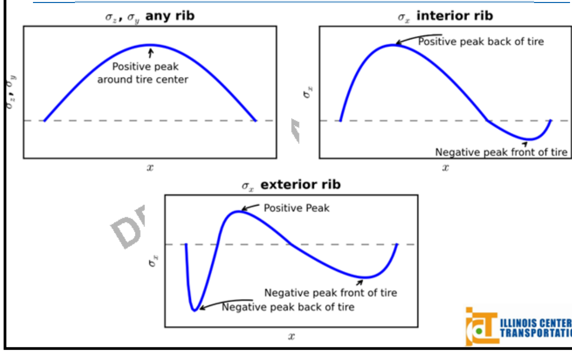


## Contact Stress Distributions

Typical Stress Distribution

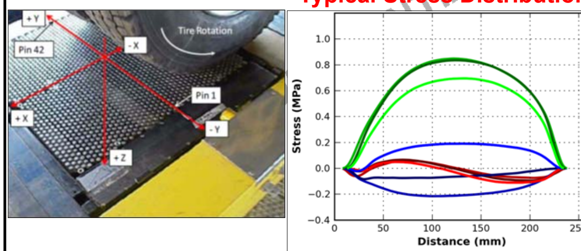


## Vertical Contact Stresses

- "n" and "m" Shape Patterns: DTA

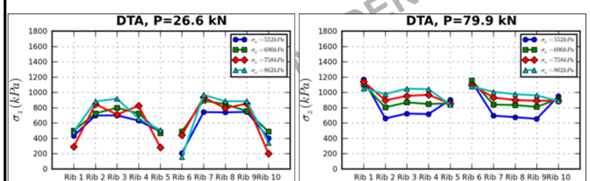


## Vertical Contact Stresses

- "n" and "m" Shape Patterns: WBT

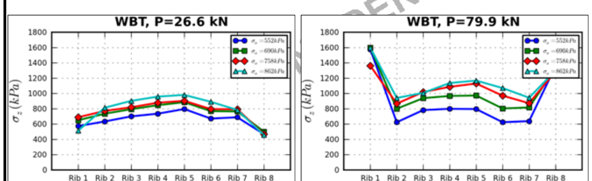


## Vertical Contact Stresses

- Effect of $\sigma_o$ on $\sigma_z$ for DTA with differential $\sigma_o$

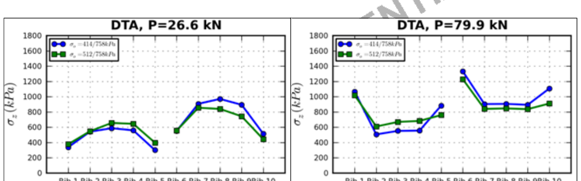


## Vertical Contact Stresses

- Normalized $\sigma_z$

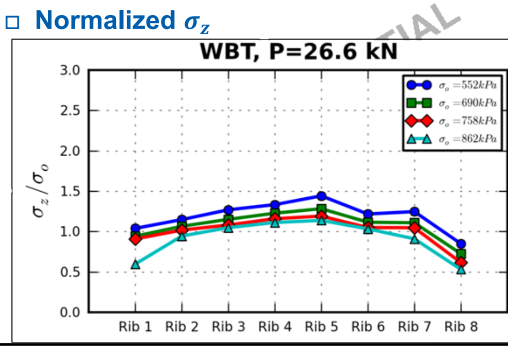

## Vertical Contact Stresses

- Normalized $\sigma_z$ for DTA with differential $\sigma_o$

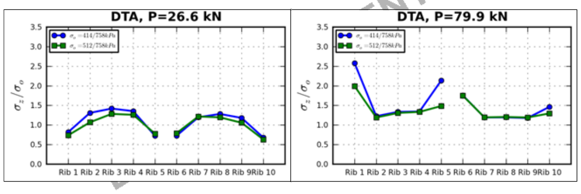


## Vertical Contact Stresses

- Maximum $\sigma_z$

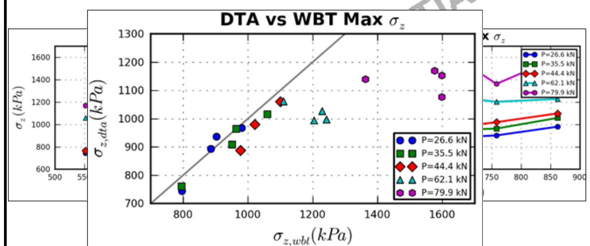


## Transverse Contact Stresses

- Maximum $\sigma_y$ for WBT

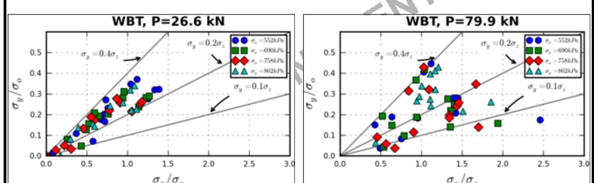


## Transverse Contact Stresses

- Maximum $\sigma_y$ for DTA

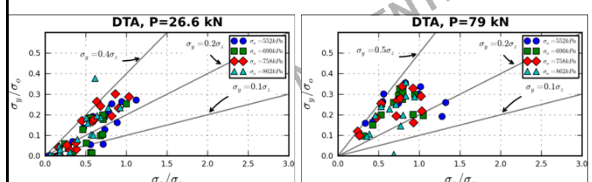


## Contact Area

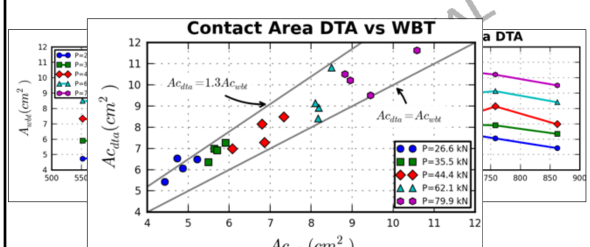


## Maximum Contact Length

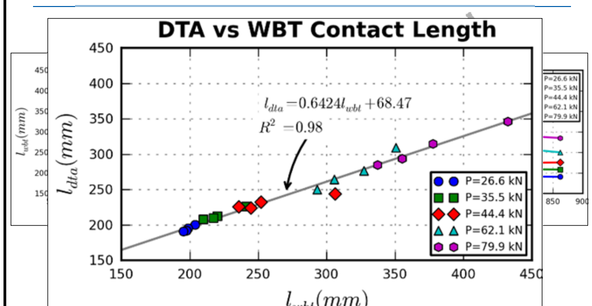

## Remarks

- Mechanisms of load transfer vary for various tires:
  - Contact **area** may be up to **30% greater** for DTA than WBT
  - Contact **length** may be up to **65% shorter** for DTA than WBT
- Complex **3D contact stresses** are important to determine pavement response
- **Robust analysis** needs to be performed in order to determine the actual **damage** caused by the two tires



## Future Plans

- Finalize detailed analysis of DTA and WBT **magnitude** and **distribution** of contact stresses
- Finalize **prediction** of contact stresses using **FEM**



## COMMENTS!



## Pavement Modeling (Delft/UIUC)

**9:15-10:00am**

5/30/2013



## TU Delft Update

TU Delft Delft University of Technology

The University of Nottingham UNITED KINGDOM · CHINA · MALAYSIA



## Outline

- Pavement Structure
- Mesh Configuration
- Loading Function
- Dual and Wide-Base Tires
- Material Characteristics
- Analysis Output
- Completed Tasks
- Future Works

## Thick Pavement Structure

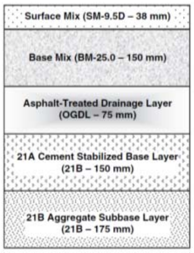


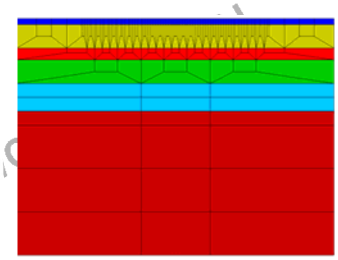

ILLINOIS CENTER FOR TRANSPORTATION

## Mesh of Thick Pavement

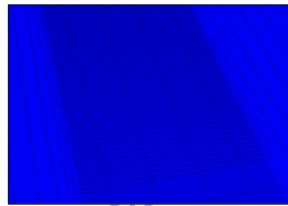

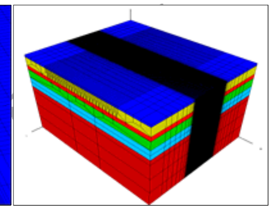

- Mesh size reduction in the depth direction provides a balance of accuracy directly under the loading area and reduced computational time
- Fine mesh in the transverse direction based on previous research from UIUC

ILLINOIS CENTER FOR TRANSPORTATION

## Sinusoidal Loading Function in CAPA-3D

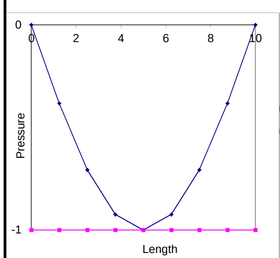


Total force calculated from the closed form solution of the integration of a sine load:

$$F=(p\ell)w=\left(-\int_0^{10}\sin\left(\frac{2\pi}{20}x\right)dx\right)\cdot 10=\left(\frac{10}{\pi}\cos\left(\frac{\pi}{10}x\right)\Big|_{x=0}^{x=10}\right)\cdot 10=$$

$$=\left(\frac{10}{\pi}\left(\cos(\pi)-\cos(0)\right)\right)\cdot 10=\frac{10}{\pi}(-1-1)\cdot 10=-\frac{200}{\pi}=-63.662$$

Sum of reaction forces in CAPA-3D for the same loading as the closed form solution = 63.671

Error of less than 0.01%

ILLINOIS CENTER FOR TRANSPORTATION

## General Form of Loading Used

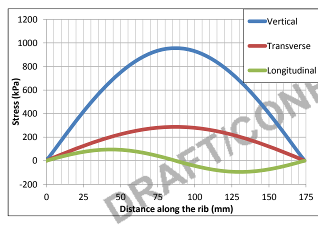


Contact stress distribution in 3D is assumed as follows:

$$\sigma_{ver} = \sigma_{max,ver}\sin\left(\frac{\pi x}{L}\right)$$

$$\sigma_{trans} = 0.3\sigma_{max,ver}\sin\left(\frac{\pi x}{L}\right)$$

$$\sigma_{long} = 0.1\sigma_{max,ver}\sin\left(\frac{2\pi x}{L}\right)$$

where,

$\sigma_{max,ver}$ = maximum vertical contact stress in the rib

$L$ = length of the rib

$x$ = distance along the rib

ILLINOIS CENTER FOR TRANSPORTATION

## Maximum Vertical Pressure & Footprint Dimensions

| | | Rib 1 | Groove 1 | Rib 2 | Groove 2 | Rib 3 | Groove 3 | Rib 4 | Groove 4 | Rib 5 |
|---|---|---|---|---|---|---|---|---|---|---|
| DTA | Vertical pressure (kPa) | 641 | 11.4 | 872 | 14.6 | 988 | 14.6 | 858 | 11.4 | 644 |
| | Length (mm) | 119 | | 153 | | 153 | | 153 | | 119 |
| | Width (mm) | 34 | | 30 | | 32.5 | | 30 | | 34 |
| WBT | Vertical pressure (kPa) | 502 | 9.6 | 832 | 9.6 | 886 | 10.3 | 936 | 11.4 | 956 |
| | Length (mm) | 136 | | 153 | | 153 | | 170 | | 170 |
| | Width (mm) | 38 | | 31 | | 31 | | 31 | | 35 |

ILLINOIS CENTER FOR TRANSPORTATION

## DTA Loading Footprint

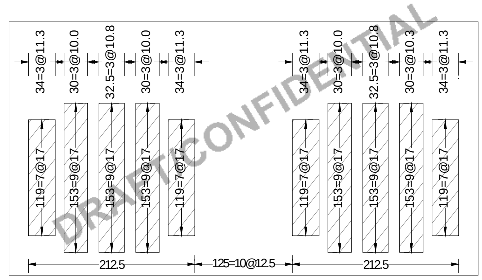


ILLINOIS CENTER FOR TRANSPORTATION

## WBT Loading Footprint

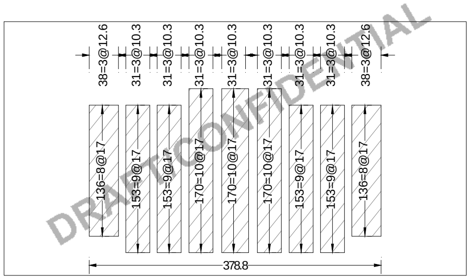


## 3D Loading on Thick Pavement Mesh

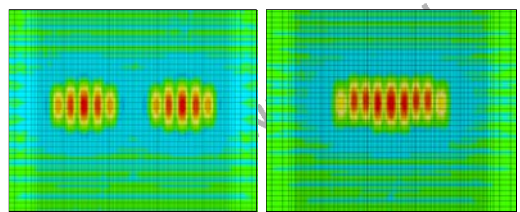

DTA WBT

## Moving DTA and WBT Loading

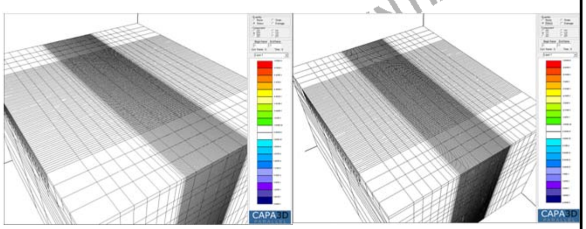

## Material Characteristics

| Layer | Modulus (MPa) | Poisson's Ratio |
|---|---|---|
| Surface Mix (SM-9.5D) | 4230.0 | 0.33 |
| Base Mix (BM-25.0) | 4750.0 | 0.30 |
| Asphalt-Treated Drainage Layer (OGDL) | 2415.0 | 0.30 |
| 21A Cement Treated Base Layer (21B) | 10342.0 | 0.20 |
| 21B Aggregate Subbase Layer (21B) | 310.0 | 0.35 |
| Subgrade | 262.0 | 0.35 |

## Surface Layer Viscoelastic Characterization

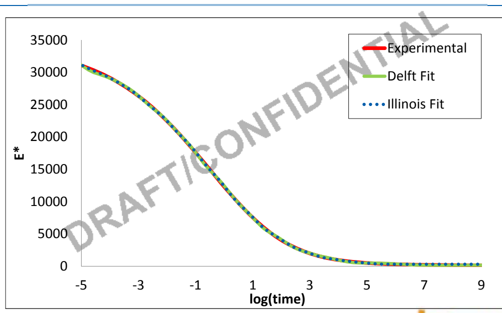


## Positions Where Outputs Are Required

- Maximum tensile strain on transverse and longitudinal directions of asphalt concrete surface.
- Maximum tensile strain on transverse and longitudinal directions at of bottom of the asphalt concrete layers.
- Maximum vertical compressive strain at top of subgrade.
- Maximum shearing strain in asphalt concrete layers: under the tire and beside the tire.

## Output from Dual and WBT Loadings

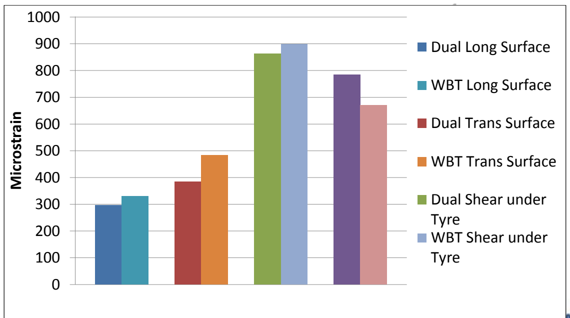


## Output from Dual and WBT Loadings

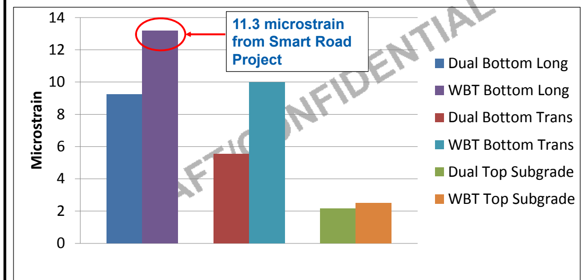




## Loading Positions for DTA Relative to Center

| Strain Label (Dual) | Depth from Surface location | Distance from Loading Center in Traveling Direction | Distance from Center of Loading in Transverse Direction |
|---|---|---|---|
| Long Surface | Surface | -78mm | -0.3mm |
| Trans Surface | Surface | -10mm | 15mm (between rib 3-4) |
| Shear under tire | 34mm | +41mm | 0.3mm |
| Shear beside tire | 34mm | +24mm | 111mm (5mm from the tire edge) |
| Bottom Long | Bottom of Asphalt | -37mm | -50mm |
| Bottom Trans | Bottom of Asphalt | -37mm | -7mm |
| Top Subgrade | Top of Subgrade | +42mm | 173mm (center of DTA) |

Note: Minus indicates a position beyond the center

## Loading Positions for WBT Relative to Center

| Strain Label (WBT) | Depth Location from Surface location | Distance from Loading Center in Traveling Direction | Distance from Center of Loading in Transverse Direction |
|---|---|---|---|
| Long Surface | Surface | -87mm | 0.6mm |
| Trans Surface | Surface | -19mm | 29mm (between rib 5-6) |
| Shear under tire | 34mm | -32mm | -0.6mm |
| Shear beside tire | 34mm | -19mm | 192mm (2mm from the tire edge) |
| Bottom Long | Bottom of Asphalt | -45mm | -0.6mm |
| Bottom Trans | Bottom of Asphalt | -45mm | -0.6mm |
| Top Subgrade | Top of Subgrade | +34mm | -0.6mm |

Note: Minus indicates a position beyond the center

## Remarks

- An **efficient** and **accurate** mesh has been developed for **CAPA-3D** per the specifications outlined by TU Delft
- Discretization of the non-uniform contact stress measurements supplied for the DTA and the WBT into a **moving 3D non-uniform contact stress** pulse.
- **Viscoelastic** model parameter determination for the surfacing layer using LTTP 26.0 data provided by UIUC. The CAPA-3D model matched the experimental and the Illinois results
- Determination of mesh locations for output of **maximum strains** at pre-agreed key locations



## Future Plans

- TU Delft will continue analysis using the contact stress matrix for DTA and WBT upon complete verification of the model
- TU Delft will proceed to produce the cloud of data needed for the **Artificial Neural Networks** tool

## COMMENTS!



TU Delft

ILLINOIS CENTER FOR TRANSPORTATION

## Pavement Modeling (UIUC)

5/30/2013



ILLINOIS CENTER FOR TRANSPORTATION

## Outline

- Finite element modeling (FEM)
  - Dynamic-implicit analysis
  - Material characterization
  - 3D contact stresses
  - Continuous moving loading
  - Infinite boundary elements
  - Layer interaction
- Mesh sensitivity analysis
- FEM analysis matrix
  - Pavement structures
  - Load cases



ILLINOIS CENTER FOR TRANSPORTATION

## Outline

- Python Development Environment
- FEM input
  - Load
  - Materials
  - Temperature
- Sample results
- Response of thin pavements
- Response of thick pavements



ILLINOIS CENTER FOR TRANSPORTATION

## Finite Element Modeling



ILLINOIS CENTER FOR TRANSPORTATION

## Dynamic-Implicit Analysis

- Considers mass inertia and damping forces effect on pavement response
- Different contact areas of tire imprint can affect inertia force values
- Pavement response is affected by loading amplitude



ILLINOIS CENTER FOR TRANSPORTATION

## Materials Characterization

- AC: Linear-Viscoelastic:
  - E* test
  - Prony Series Expansion
- Granular Materials:
  - Thin Pavement: Nonlinear stress-dependent
  - Thick Pavement: Linear Elastic

## 3D Contact Stresses

- Uniform constant stresses underestimate response close to the surface
- 3D contact stresses may create greater compressive strain on top of subgrade and transverse tensile strain

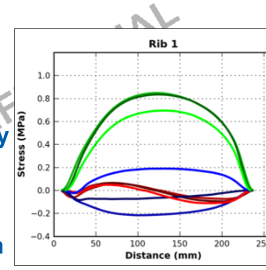


## Continuous Moving Loading

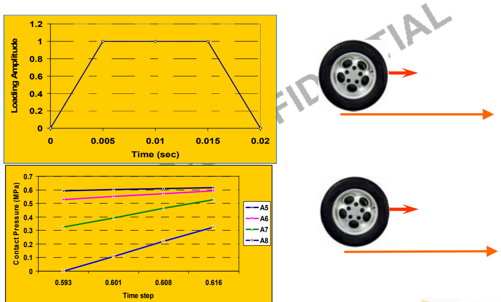


## Finite Element Model

- Infinite Boundary Elements
  - Simulates far-field region
- Layer Interaction:
  - Fully-bonded
  - Simple Friction
  - Elastic Slip

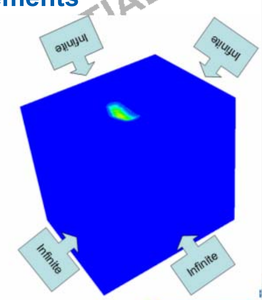


## Mesh Sensitivity Analysis

## Mesh Sensitivity Analysis

- Optimum (computational- and accuracy-wise) distribution and location of finite elements
- Parametric study in Abaqus using BISAR as reference
- Responses compared: tensile strains at bottom of AC; shear strain in each layer; and vertical strain on top of subgrade
- 5% difference used as criteria for optimum mesh
- Mesh in plan view defined by tire's footprint and transition to model's boundary

# Mesh Sensitivity Analysis

- Model parameters in plan view

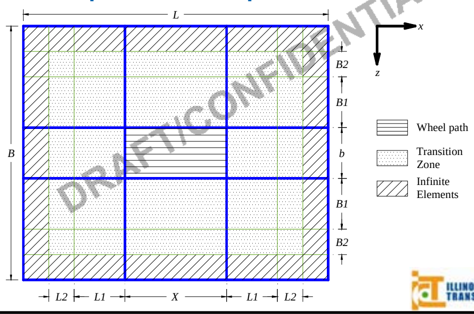


# Mesh Sensitivity Analysis

- Two-step approach

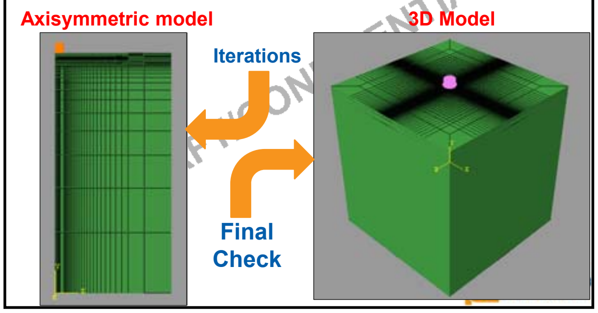


# Mesh Sensitivity Analysis

- Abaqus (3D) vs. BISAR: thin pavements

| | AC=75 mm, Base=150 mm | | | AC=75 mm, B=600 mm. | | | AC=125 mm, Base=150 mm | | | AC=125 mm, Base=600 mm | | |
|---|---|---|---|---|---|---|---|---|---|---|---|---|
| | Abaq. | BIS. | Dif.* | Abaq. | BIS. | Dif.* | Abaq. | BIS. | Dif.* | Abaq. | BIS. | Dif.* |
| $\varepsilon_{11,ac}$ | 126.5 | 133.8 | 5.5 | 105.4 | 111.3 | 5.3 | 63.9 | 67.2 | 4.9 | 56.6 | 59.5 | 4.9 |
| $\varepsilon_{22,subg}$ | 817.9 | 836.8 | 2.3 | 354.6 | 364.4 | 2.7 | 341.0 | 348.9 | 2.3 | 206.5 | 212.6 | 2.9 |
| $\varepsilon_{23,ac}$ | 27.0 | 27.4 | 1.4 | 25.5 | 26.1 | 2.3 | 17.0 | 17.0 | 0.2 | 16.4 | 16.5 | 0.7 |
| $\varepsilon_{23,base}$ | 193.0 | 190.4 | 1.4 | 179.1 | 170.7 | 4.9 | 68.4 | 67.9 | 0.8 | 75.2 | 73.0 | 3.0 |
| $\varepsilon_{23,subg}$ | 269.9 | 276.6 | 2.4 | 128.7 | 135.1 | 4.8 | 101.6 | 103.9 | 2.2 | 70.6 | 75.8 | 6.9 |

*Difference in %

# Mesh Sensitivity Analysis

- Abaqus (3D) vs. BISAR: thick pavements

| | AC=125 mm, Base=150 mm | | | AC=412 mm, Base=600 mm | | | AC=125 mm, B=150 mm | | | AC=412 mm, Base=600 mm | | |
|---|---|---|---|---|---|---|---|---|---|---|---|---|
| | Abaq. | BIS. | Dif.* | Abaq. | BIS. | Dif.* | Abaq. | BIS. | Dif.* | Abaq. | BIS. | Dif.* |
| $\varepsilon_{11,ac}$ | 65.6 | 68.1 | 3.7 | 61.1 | 63.8 | 4.2 | 9.9 | 9.4 | 5.2 | 9.1 | 9.7 | 6.3 |
| $\varepsilon_{22,subg}$ | 300.0 | 295.5 | 1.5 | 157.4 | 159.7 | 1.4 | 36.0 | 36.1 | 0.3 | 27.9 | 27.8 | 0.3 |
| $\varepsilon_{23,ac}$ | 19.4 | 19.2 | 1.0 | 19.8 | 19.4 | 1.8 | 7.3 | 7.6 | 4.0 | 7.6 | 7.3 | 4.2 |
| $\varepsilon_{23,base}$ | 73.3 | 70.0 | 4.7 | 74.9 | 74.7 | 0.3 | 6.8 | 6.6 | 3.3 | 7.9 | 8.0 | 1.3 |
| $\varepsilon_{23,subg}$ | 83.2 | 88.2 | 5.7 | 53.7 | 56.6 | 5.1 | 8.5 | 8.1 | 5.0 | 7.8 | 8.2 | 4.8 |

*Difference in %

# Mesh Sensitivity Analysis

- Final configuration thin pavement:

| Thin Pavements | | Model | | | |
|---|---|---|---|---|---|
| | | AC=75 mm, Base=150 mm | AC=75 mm, Base=600 mm | AC=125 mm, Base=150 mm | AC=125 mm, Base=600 mm |
| Dimensions (mm) | $L$ | 4300 | 5800 | 4800 | 5300 |
| | $B$ | 4300 | 5800 | 4800 | 5300 |
| | $D$ | 4500 | 4500 | 4500 | 4500 |
| | $L1 = B1$ | 1200 | 1950 | 1450 | 1700 |
| | $L2 = B2$ | 300 | 300 | 300 | 300 |
| AC | No. Elem. | 12 | 12 | 15 | 15 |
| | Bias | 1.0 | 1.0 | 1.2 | 1.2 |
| Base | No. Elem. | 12 | 25 | 12 | 25 |
| | Bias | 1.7 | 1.3 | 1.7 | 1.0 |
| Subgrade | No. Elem. | 15 | 15 | 15 | 15 |
| | Bias | 70.0 | 30.0 | 50.0 | 30.0 |
| $L1 = B1$ | No. Elem. | 25 | 30 | 30 | 25 |
| | Bias | 10.0 | 20.0 | 10.0 | 15.0 |
| $L2 = B2$ | No. Elem. | 1 | 1 | 1 | 1 |
| | Bias | 1.0 | 1.0 | 1.0 | 1.0 |

# Mesh Sensitivity Analysis

- Final Model

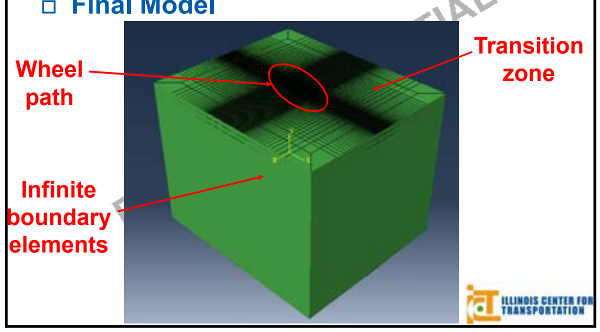

# FEM Analysis Matrix





# FEM Analysis Matrix

- Structures considered: Thin pavement

| Thin Pavement Structure | | |
|---|---|---|
| | Different Materials | Thicknesses |
| **AC Layer** | W, S* | 75 and 125 mm |
| **Base** | W, S* | 150 and 600 mm |
| **Subgrade** | 35 and 140 MPa | -- |
| **Possible combination** | 32 | |
| **With load cases (12)** | 384 | |

*W = Weak; S = Strong



# FEM Analysis Matrix

- Structures considered: Thick pavement

| Thick Pavement Structure | | |
|---|---|---|
| | Different Materials | Thicknesses |
| **Wearing Surface** | W1, S1* | 25 and 62.5 mm |
| **Intermediate Layer** | W2, S2* | 37.5 and 100 mm |
| **Binder Layer** | W3, S3* | 62.5 and 250 mm |
| **Base and Subbase** | 140 and 415 MPa | 150 and 600 mm |
| **Subgrade** | 70 MPa | -- |
| **Possible Combination** | 16 | |
| **With Load cases (12)** | 192 | |

*W = Weak; S = Strong



# FEM Analysis Matrix

- Loading Cases

| Load Case | Tire Type | Applied Load (kN) | Tire Inflation Pressure (kPa) |
|---|---|---|---|
| **L1** | WBT | 26.6 | 552 |
| **L2** | WBT | 26.6 | 862 |
| **L3** | WBT | 79.9 | 552 |
| **L4** | WBT | 79.9 | 862 |
| **L5** | DTA | 26.6 | 552 |
| **L6** | DTA | 26.6 | 862 |
| **L7** | DTA | 26.6 | 562/758 |
| **L8** | DTA | 79.9 | 562 |
| **L9** | DTA | 79.9 | 862 |
| **L10** | DTA | 79.9 | 562/758 |
| **L11** | WBT | 44.4 | 758 |
| **L12** | DTA | 44.4 | 758 |



# Pavement Modeling (Thin & Thick)

**10:15-11:00am**

5/30/2013





# Abaqus Python Development Environment (PDE)

# Abaqus PDE

- Abaqus PDE*
  - Automate repetitive tasks
  - Perform parametric studies
  - Create and modify models
  - Access data in an output database

*Abaqus 6.11 Documentation

# Generation of Input Files (Abaqus PDE)

- Geometry and materials: Model dimensions, layer thicknesses, material definition, and layer interaction
- Mesh: element type and size in each layer, mesh configuration in tire's footprint, and transition to model boundary
- Load: 3D contact stresses in footprint, continuous moving load, temperature

# Abaqus PDE

- Extract information from output database (post-processing):
  - Extreme responses in each layer
  - Locations of responses
  - Variation of responses along paths (e.g. depth)

# FEM Input

# FEM Input

- Load: Contact stress measurements
- AC materials: LTPP Database
- Granular materials: Nonlinear cross-anisotropic laboratory characterization
- Temperature profile: Analytical temperature distribution model

# FEM Input

- Load

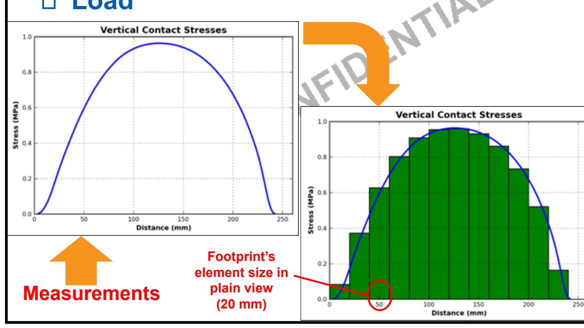

## FEM Input

- From **measurements** to **FEM**

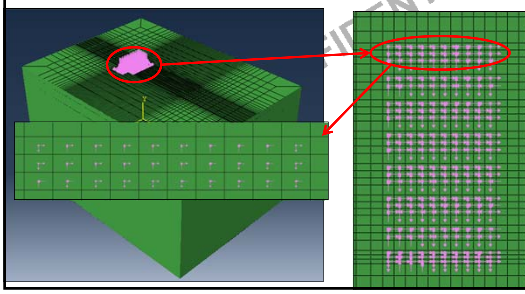




## FEM Input

- AC Materials
  - Long-Term Pavement Performance (**LTPP**) Data Release #26
    - Two sets representing the **extreme limits** → (a) weak and (b) strong
  - Methodology
    - **Statistical** Analysis
    - **NMAS** Criterion (typical values per layer)



## FEM Input

- Based on more than **1000 data sets**

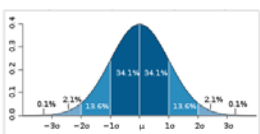


$2\sigma \approx 95.4\%$, $2.5\sigma \approx 97.5\%$ and $3\sigma \approx 99.8\%$

- Layer Properties: **NMAS**
  - Wearing Surface (WS) 9.5 or 12.5mm
  - Intermediate Layer (IS) 25 or 19.5mm
  - Base Layer (BS) 25 or 37.5mm

From http://en.wikipedia.org/wiki/Normal_distribution.



## FEM Input: AC Materials

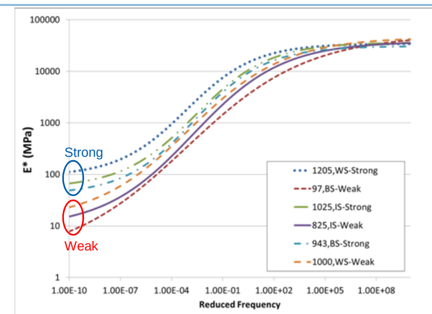


## FEM Input

- Base materials (**thin** pavements)
  - **Cross-anisotropic stress-dependent**

$$M_r = k_1 p_a \left(\frac{\theta}{p_a}\right)^{k_2} \left(\frac{\tau_{oct}}{p_a} + 1\right)^{k_3}$$

  - Based on database of **114 materials** (Tutumluer, 2008)
  - Materials in database tested using **pulse load** in **vertical** and **radial** directions



## FEM Input

- Two stress levels defined to select weak and strong material (Xiao et al., 2011)

| | Low stress level | High stress level |
|---|---|---|
| | kPa | kPa |
| $\sigma_3$ | 34.9 | 104.8 |
| $\sigma_d$ | 104.8 | 209.5 |
| $\sigma_1$ | 139.7 | 314.3 |
| $\sigma_2$ | 34.9 | 104.8 |
| $\theta$ | 209.5 | 523.9 |

# FEM Input

- Vertical resilient modulus of each material at both stress levels

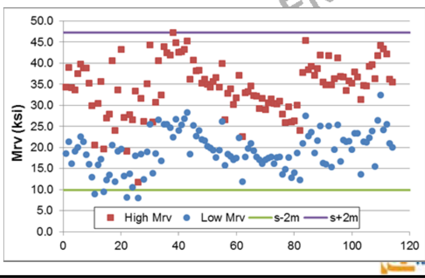


# FEM Input

- Vertical and horizontal shear modulus from laboratory tests
- Shear resilient modulus from simplified procedure (Tutumluer and Thompson, 1998)

| Direction | Weak | | | Strong | | |
|---|---|---|---|---|---|---|
| Vertical | $k_1$=453.3 | $k_2$=0.8858 | $k_3$=-0.5713 | $k_1$=869.6 | $k_2$=0.9785 | $k_3$=-0.5673 |
| Horizontal | $k_4$=282.4 | $k_5$=0.6701 | $k_6$=-1.1341 | $k_4$=596.6 | $k_5$=1.1419 | $k_6$=-1.3464 |
| Shear | $k_7$=310.3 | $k_8$=1.0297 | $k_9$=-1.1036 | $k_7$=389.1 | $k_8$=0.9083 | $k_9$=-0.2409 |

# FEM Input

- Temperature distribution in AC (Wang, 2013)
  - Two layer system: AC layers and granular
  - Bound temperature distribution
  - Initial temperature distribution function of depth $z$ only
  - Continuous heat flow at the interface between layers



# Temperature Distribution

- Governing Equations
  - Temperature distribution in each layer:

$$\frac{\partial T_1}{\partial t}(z,t) = \alpha_1 \frac{\partial^2 T_1}{\partial z^2}(z,t) \qquad 0 < z < H$$

$$\frac{\partial T_2}{\partial t}(z,t) = \alpha_2 \frac{\partial^2 T_2}{\partial z^2}(z,t) \qquad z > H$$

  - Initial temperature in each layer:

$$T_1(z,0) = G_1(z) \qquad 0 < z < H$$

$$T_2(z,0) = G_2(z) \qquad z > H$$



# Temperature Distribution

- Continuous temperature and heat flow at interface:

$$T_1(H,t) = T_2(H,t)$$

$$\lambda_1 \frac{\partial T_1}{\partial z}(H,t) = \lambda_2 \frac{\partial T_2}{\partial z}(H,t)$$

- Energy Balance at pavement surface:

$$\lambda_1 \frac{\partial T_1}{\partial z}(0,t) = B[T(t) - T_1(0,t)]$$



# Temperature Distribution

- Solution for AC layer:

$$\hat{U}_1(z,s) = \frac{B\hat{f}(s)\left[e^{\sqrt{\frac{s}{\alpha_1}}z} - Le^{(2H-z)\sqrt{\frac{s}{\alpha_1}}}\right]}{B - \lambda_1\sqrt{\frac{s}{\alpha_1}} - e^{2H\sqrt{\frac{s}{\alpha_1}}}L\left(B + \lambda_1\sqrt{\frac{s}{\alpha_1}}\right)};$$

$$\text{with } L = \frac{1 + \frac{\lambda_1 r_1}{\lambda_2 r_2}}{1 - \frac{\lambda_1 r_1}{\lambda_2 r_2}}$$

# Temperature Distribution

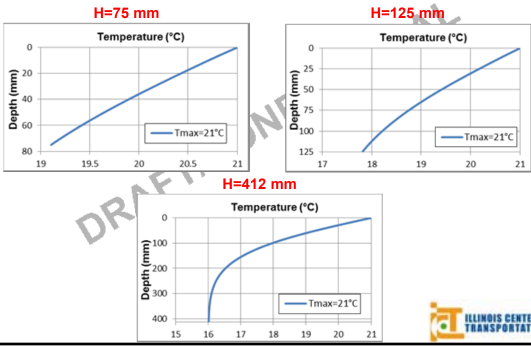


# Sample of Results



# Sample of Results

- For each one of the **576 cases**

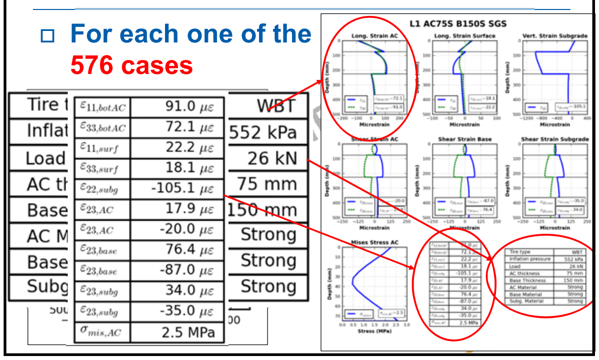


# Sample of Results

L1 AC75S B150S SGS

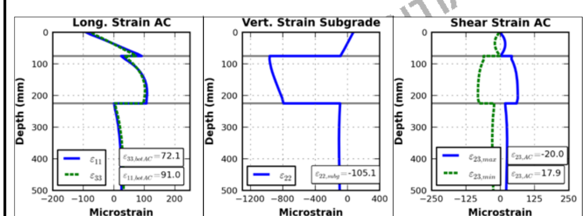


# Responses of Thin Pavements

# Responses of Thin Pavements

- **Thinnest pavement (AC=75 mm and Base=150 mm) all material combinations:**
  - WBT vs. DTA at low load and tire-inflation pressure (P=26.6 kN, σ=552 kPa)
  - WBT vs. DTA at high load and tire-inflation pressure (P=79.9 kN, σ=862 kPa)
- **All load combinations for the same pavement structure**

## Strain at the bottom of AC

AC75 B150

P=26.6 kN, σ=552 kPa

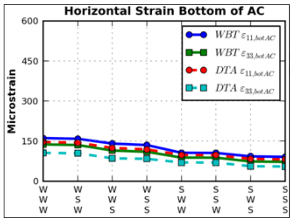


P=79.9 kN, σ=862 kPa

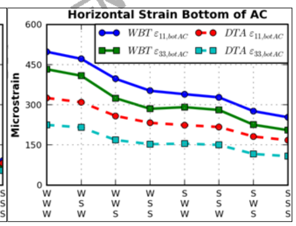


## Effect of Loading Cases

- Tensile strain at bottom of AC

AC75S B150W SGW

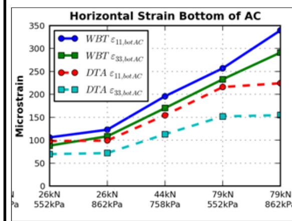


Weak Subgrade

AC75S B150W SGS

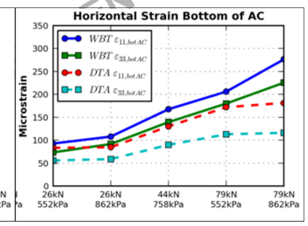


Strong Subgrade

## Responses of Thick Pavement

## Responses of Thick Pavements

- Thinnest pavement (AC=125 mm and Base=150 mm) all material combinations:
  - WBT vs. DTA at low load and tire-inflation pressure (P=26.6 kN, σ=552 kPa)
  - WBT vs. DTA at high load and tire-inflation pressure (P=79.9 kN, σ=862 kPa)
- All load combinations for the same pavement structure (AC=412 mm and Base=150 mm)

## Effect of Material Properties

AC125 B150

P=26 kN, σ=552 kPa

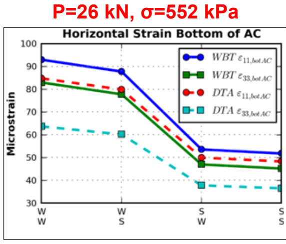


P=79 kN, σ=862 kPa

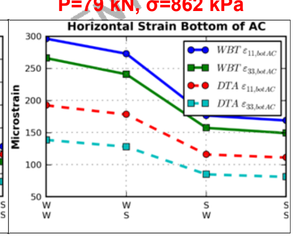


## Effect of Loading Cases

AC412S B150W

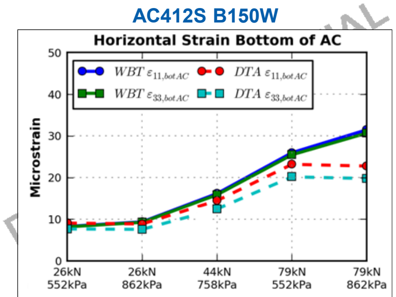

## Remarks

- Small difference between horizontal strains in the longitudinal and lateral directions (top and bottom of AC)
- Difference between WBT and DTA become more pronounced with higher load and higher tire pressure



## Future Plans

- Complete thin and thick pavement cases with various combinations of axle loads and tire inflation pressures
- Provide comprehensive analysis with regards to the effect of:
  - Tire type
  - Material property
  - Loading case
  - Pavement structure



## COMMENTS!



## Data Management
## 11:00-12:00am

5/30/2013



## Outline

- Introduction and Objectives
- Existing data
- New data
- Filtering process
- Interface design
- Future Plans: Artificial Neural Network



## The Need for Field and APT Data

- Represent real conditions
- Realistic responses from field
- Model validation
- Utilize as training or for the testing phase of Artificial Neural Networks

## Objectives of Data Management

- Data filtering as needed and process automation
- Data management and organization
- Allow easy access to data by designing an interface
- Provide a platform for future data updates



## Data Sources

- Five main data sources:
  - UIUC-Thin Pavement Sections
  - Florida DOT
  - UC-Davis
  - Ohio SPS-8
  - Virginia Tech - Smart Road
- Huge amount of data/information
- Update w/ new data as it becomes available



## UIUC-Thin Pavement Sections

- Nine low-volume AC sections
- Three tire types: Dual, WBT-425, and WBT-455
- Various loads, speeds, and tire inflation pressures
- Instrumentation: Strain gauges, LVDT, pressure cells, and thermocouples



## UIUC-Thin Pavement Sections-Data

- Strain at the bottom of surface layer
- Vertical deflection on top of subgrade
- Longitudinal and transverse base deformations
- Surface rutting



## Florida DOT

- Six test lanes
- Open- and dense-graded AC layers
- Tires: Dual, WBT-445, WBT-455
- Instrumentation: Surface strain gauges (longitudinal and transverse)
- Rutting data



## UC-Davis

- Rutting of two overlay systems: dense-graded AC (DGAC) and asphalt-rubber hot mix gap-graded (ARHM-GG)
- Tire types: Dual radial, dual bias-ply, WBT-425, and aircraft tires
- Profile data
- 3D contact stresses

## Ohio SPS-8

- Two sections of 4- and 8-in-thick AC on the U.S. Route 23 Test Road
- Single-unit two axle truck with two tires: Two dual and two wide-base (WBT425, WBT495)
- Strain gage rosettes in different directions at AC layer
- Tire pressure patterns
- FWD



ILLINOIS CENTER FOR TRANSPORTATION

## Virginia Tech Smart Road

- 1999-2002 database
- Instrumentation: Strain gauges (AC, base, sub-base); Pressure cells (two types); Time-domain reflectometry (TDR), thermocouples, …
- Dynamic data response
- Static environmental data response
- GPR, friction, roughness, and FWD



ILLINOIS CENTER FOR TRANSPORTATION

## New Data Sources

- Florida DOT
- UC-Davis
- Ohio



ILLINOIS CENTER FOR TRANSPORTATION

## Florida DOT

- Test Pit and Test Track data
- Dual and NGWB tires
- Instrumentation: Embedded and surface strain gauges
- Pressure cells (bottom of AC and base)



ILLINOIS CENTER FOR TRANSPORTATION

## Florida DOT – Test Matrix

| Tire Type | Inflation Pressure (kPa) | Tire Loading (kN) | | | | |
|---|---|---|---|---|---|---|
| NGWB and Dual | 552 | 26.6 | 35.5 | 44.4 | 62.2 | 79.9 |
| NGWB and Dual | 690 | | | | | |
| NGWB and Dual | 758 | | | | | |
| NGWB and Dual | 862 | | | | | |
| Dual Only | 414/758* | | | | | |
| Dual Only | 552/758* | | | | | |

*Differential Tire Inflation Pressure

ILLINOIS CENTER FOR TRANSPORTATION

## UC-Davis

- 5-in high RAP surface layer and 2-in AC wearing surface layer
- Strain gauges in both directions under the AC layer lifts
- Instrumentation: Longitudinal and transverse strain gauges (bottom of AC and RAP base layers)
- Pressure cells at bottom of aggregate base layer
- Multi-Depth Deflectometer (MDD)



ILLINOIS CENTER FOR TRANSPORTATION

# Ohio

- Total of **three sections** (mainline and ramp)
- Test matrix includes:
  - Two tire type (dual and wide)
  - Two axles (single and tandem)
  - Various loads, speeds and tire inflation pressures
- Instrumentation: Two types of **strain gauges**, **Rosettes**, two types **pressure cells**, and **LVDTs**
- Collected data to date: 3 sections out of 4 at **highest load case** (**6** out of **48** cases - **10%** completed)

# Data Filtering Process

- **Florida** and **Ohio** data filtering is in progress
- Three-step filtering process:
  - **Transferring data to origin**
  - **Smoothing/filtering** using Robust Local Regression Method
  - Extracting **local extrema**
- All processes are done in **Matlab**

# Typical Strain Data - Ohio

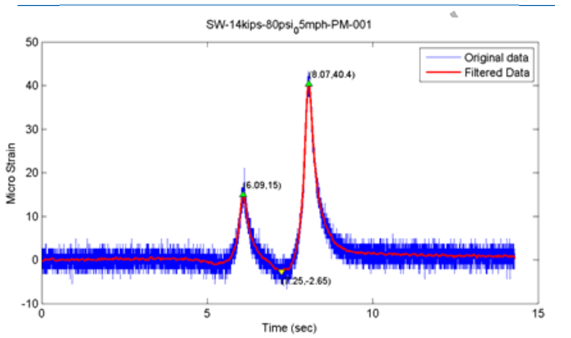


# Typical Strain Data - Florida

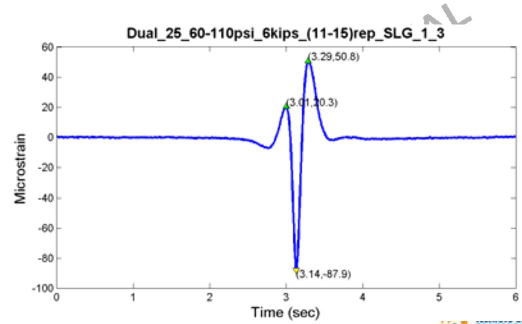


# Interface Design

- Data organization for easy access
- AutoPlay Media Studio 8 software

Run Demo

# Future Plans: Artificial Neural Network

- All useful collected **data** will be utilized
- To **predict pavement damage** caused by various **loading** and **tire configurations**
- Robust, nonlinear, and strong modeling technique
- **Accurate** if trained properly
- **Easier to use** compared to FEM
- Less computational time

## Artificial Neural Networks Input

- Pavement structure characteristics: number of layers, thicknesses, binder, elastic modulus, agg. properties, etc.
- Loading, tire configuration, and speed
- Data include: FEM, field, and APT data
  - FEM modeling data will be used for training
  - Field and APT data for validation purposes

## Artificial Neural Networks Output

- Responses related to fatigue, rutting and thermal cracking;
  - Transverse strain at bottom of AC
  - Vertical strain (deformation) on top of subgrade
- Damage Ratio

## COMMENTS!

## Laboratory Testing

**1:00-1:45pm**

5/30/2013

## Laboratory Testing

- Sampling Overview
  - Sampling
  - Splitting
  - Compacting
  - Loose Mix, MRL, etc
  - Tracking of trucks
- Cutting & Coring
- Testing

## "Mobilized" Lab

147

ILLINOIS CENTER FOR TRANSPORTATION

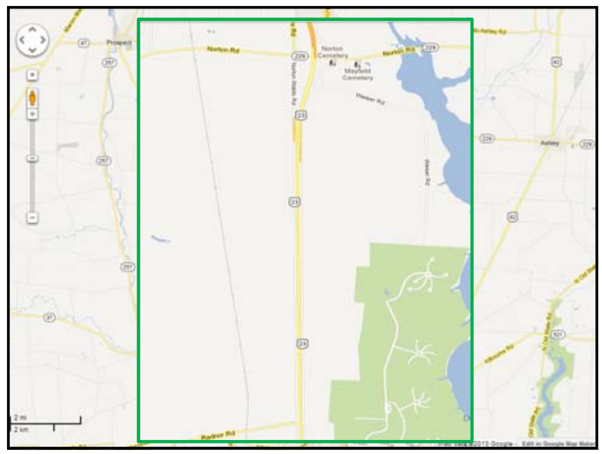

149

## Paving Sequence

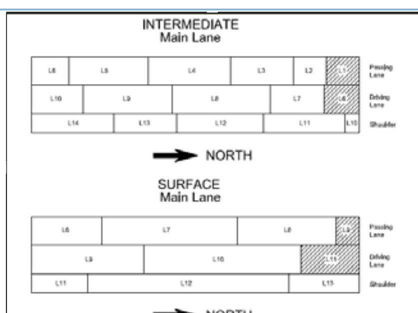


ILLINOIS CENTER FOR TRANSPORTATION

150

## Target Density

ILLINOIS CENTER FOR TRANSPORTATION

## Specimen Allocation

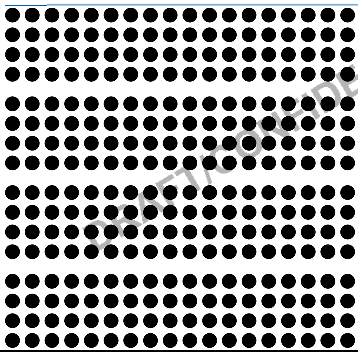




## Specimen Allocation

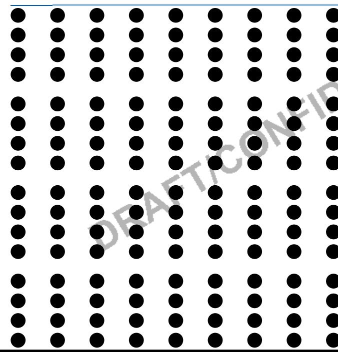




## Specimen Allocation

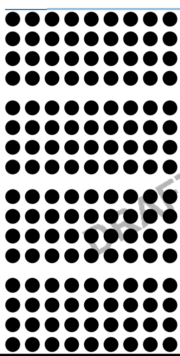




## Specimen Allocation

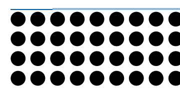




## Specimen Allocation

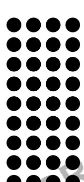

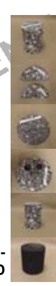




## E* Fabrication

150mm→100mm

Top/Bottom cuts

## E* Specification

- AASHTO T 342-11 (formerly TP 62-07)
  - NMAS < 37.5 mm
    - Dense- or gap-graded
  - Conditions:
    - 5 temperatures
      - -10, 4.4, 21, 38, 54 °C
      - (14, 40, 70, 100, 130 °F)
    - 6 frequencies
      - 25, 10, 5, 1, 0.5, 0.1 Hz
  - Stress-controlled test
  - Haversine axial compressive load

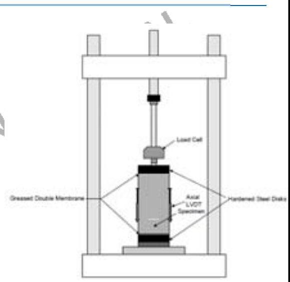




## E* Testing

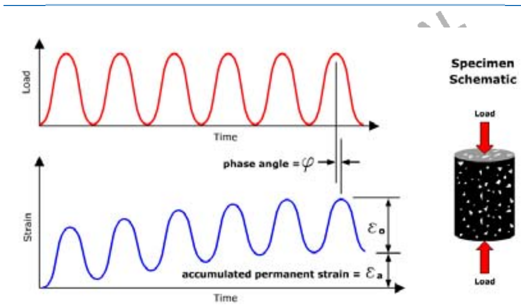


Courtesy of pavementinteractive.org

## E* Testing Images



## IDT Fabrication

50mm Slice



## IDT Specification

- ASTM D 6931-12
  - Tensile strength
  - Constant vertical deformation
  - 25 ± 1°C
- AASHTO T 322-07
  - Tensile creep
    - Static Load
      - Limited by strain
    - -20, -10, and 0 ± 0.5°
    - 3 ± 1 hrs

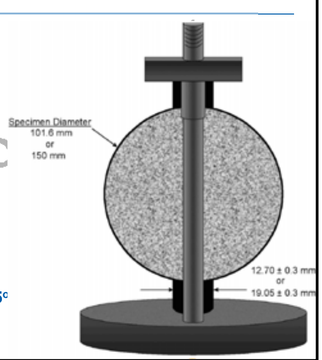




## IDT Testing Images

## SCB Fabrication


25-50mm Slice


Top/Bottom cuts


Notch

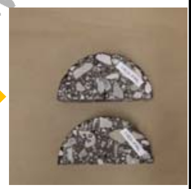

## SCB Specification

- AASHTO Draft
  - Displacement control
    - CMOD
      - 0.0005 mm/s
      - 0.03 mm/min
  - Low PG + 10°C
  - Conditioning time = 2 ± 0.2 hrs
    - Temp. = ± 1°C

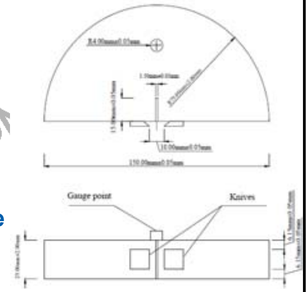

## SCB Testing Images

## DC(T) Fabrication


50mm Slice


Front Face Cut


Core Drilled Holes


Notch

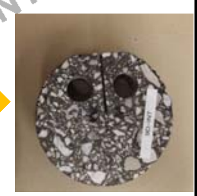

## DC(T) Specification

- ASTM D 7313
  - Test developed in 2005
  - Advantages
    - Provides larger ligament length than SCB
    - Easier geometry than SEB to fabricate from field cores
  - Displacement controlled test
    - 1.0mm/min
  - Required equipment
    - Load cell with capable resolution
    - Crack mouth opening displacement (CMOD) gauge
  - Low PG + 10°C

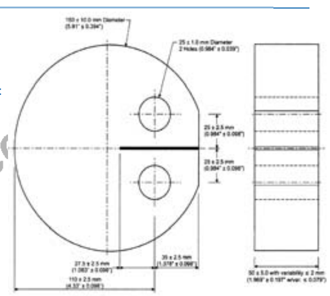

## DC(T) Testing Images

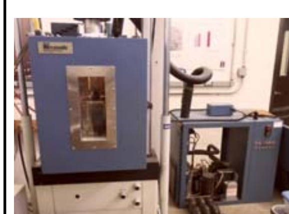

## Push-Pull Fabrication

150mm→100mm

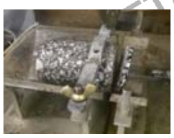

Top/Bottom cuts

## Push-Pull Specification

- Draft
  - Fatigue test
  - Continuum damage characteristics
  - Simple Uniaxial test
  - 15 & 20 ± 0.5°C

## Push-Pull Testing Images


## Equilibration Time


## This is Characterization…

- Constant target **density**, regardless of field data
- Allows for cataloging to a **vast database** with other materials that have undergone general characterization
- Monitors **consistency** of production truck-by-truck

## Density Results

- Useful to carry into validation phase

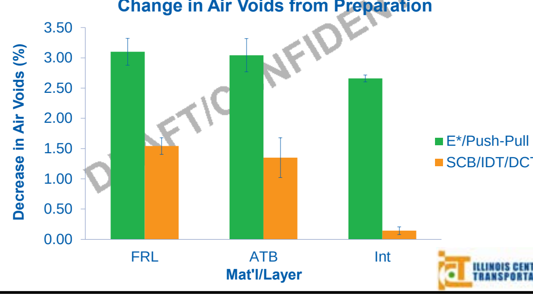

## Validation

- Loose mix collected during production will be compacted to match the nuclear density data from the field at time of placement (no longer 7.0 ± 0.5%)
- Allows for direct comparison, validation of models

(%AV: FRL=4.5, ATB=4.6, INT=4.5, SURF=4.7)







## Laboratory Testing Progress

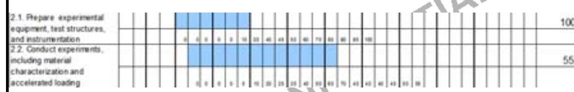


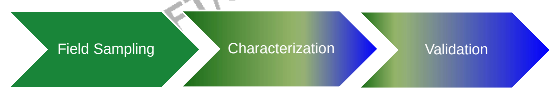








## Adjustments for Field Cores

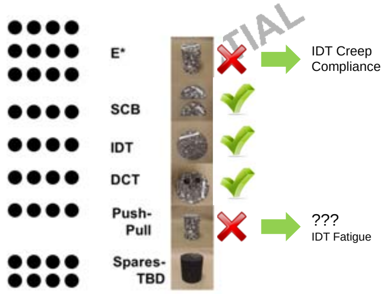


***Note: Both FL & UC-Davis will be performing E* testing on SGC specimens







## Future Plans

- Compact **SGC** specimens that **simulate** the **field**-compacted samples (air void validation)
- Finish **laboratory test matrix** for materials in all testing sites





## COMMENTS!





## Instrumentation and Testing: Ohio, Florida, and Davis

**1:45-3:15pm**

5/30/2013

# Instrumentation and Testing: Florida







## Topics

- FDOT's APT Facility
- Test Section Design
- Instrumentation
- Construction
- Material Sampling
- HVS Testing







## FDOT's APT Facility

- State Materials Research Park, Gainesville
- Test sections
  - Eight test tracks
  - Two test pits
- Heavy Vehicle Simulator (HVS)







## Test Tracks








## Test Pits

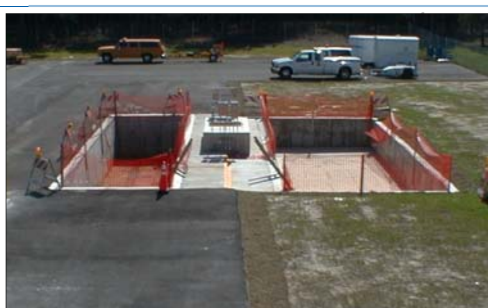





## Test Track Aerial View

# Heavy Vehicle Simulator

- Heavy Vehicle Simulator, Mark IV
  - Wheel speed: 7 mph
  - Loading: 7 to 45 kips
  - Dual or single tires




# Heating System

- Six 9 ft. long elements attached to HVS test beam
- Independently controlled to provide six heating zones
- Thermocouples monitor asphalt temperature to a depth of 2 in
- Styrofoam filled panels insulate the test area

# Test Section Design

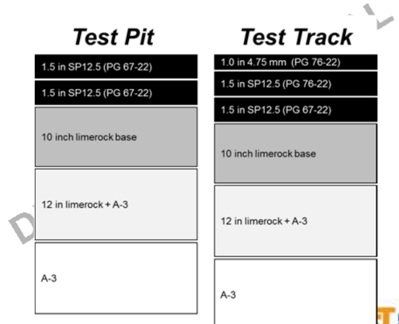


# Test Pit Instrumentation

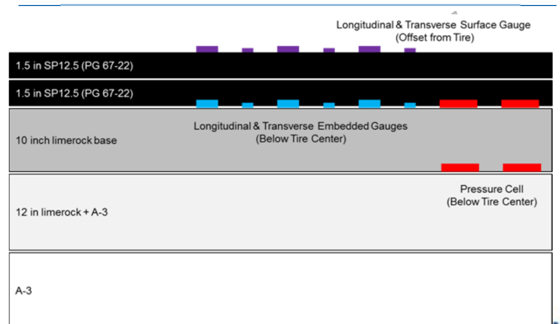


# Test Track Instrumentation

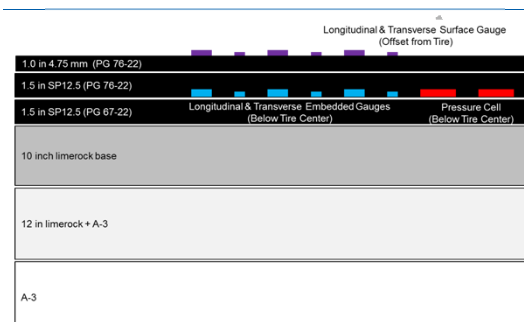


# Surface Strain Gauges

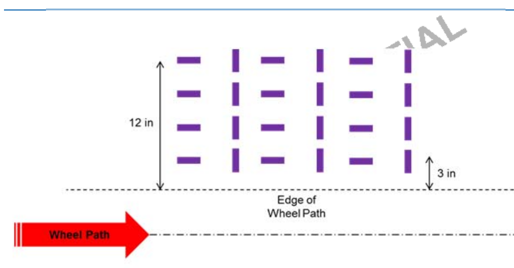

## Instrumentation Summary

| Sensor Type | Number of Sensors per Test Section | Model | Vertical Location | Offset from Wheel Path |
|---|---|---|---|---|
| Surface strain gauge | 24 | Tokyo Sokki PFL-30-11-5L | HMA surface | Transverse and longitudinal orientations at various offsets from wheel path edge |
| Asphalt strain gauge | 6 | Tokyo Sokki KM-100HAS | Bottom of new HMA | Transverse and longitudinal orientations below tire center |
| Pressure cell | 2 | RST Instruments LPTPC09-S | Bottom of new HMA | Below tire center |
| Pressure cell (Test Pit only) | 2 | Geokon 3500 | Bottom of base | Below tire center |

## Pressure Cells

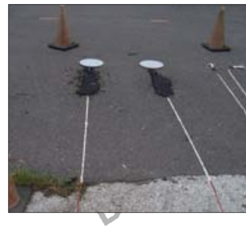

## Asphalt Strain Gauges (H-Gauges)

## Asphalt Surface Strain Gauges (Foil)

## Surface Strain – Dual Tire at 55°C

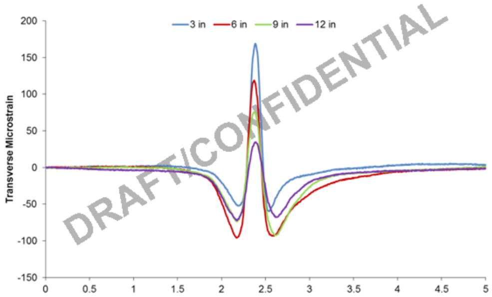


## Test Pit Construction

## Test Pit Paving

## Test Track Paving

## Material Sampling

## Laboratory Testing

- Granular Materials
  - Resilient modulus
  - Moisture-density relationship
- HMA
  - Cores
    - Verification of density
    - Cores to University of Illinois
  - Loose mixture
    - Volumetric data
    - IDT
    - AMPT



## HVS Test Matrix

| Tire Type | Inflation Pressure (psi) | Tire Loading (kips) | | | | |
|---|---|---|---|---|---|---|
| NGWB and Dual | 80 | 6 | 8 | 10 | 14 | 18 |
| NGWB and Dual | 100 | 6 | 8 | 10 | 14 | 18 |
| NGWB and Dual | 110 | 6 | 8 | 10 | 14 | 18 |
| NGWB and Dual | 125 | 6 | 8 | 10 | 14 | 18 |
| Dual Only | 60/110 | 6 | 8 | 10 | 14 | 18 |
| Dual Only | 80/110 | 6 | 8 | 10 | 14 | 18 |

Tests at 25°C, 40°C, and 55°C

## Completed Tasks

- The construction, instrumentation, and testing at Florida has been completed

## COMMENTS!





## Instrumentation and Testing: California

UCDAVIS
UNIVERSITY OF CALIFORNIA





## Completed Tasks

- HVS response testing on two flexible pavements
  - Status: Completed
- Prelimi[...] (CA) for energy [...] n house gas) em[...]
  - Status[...]

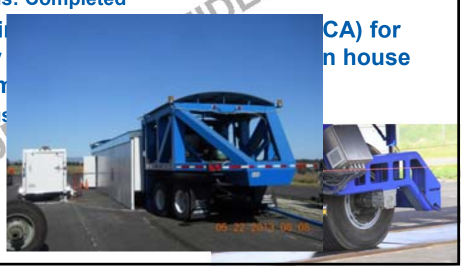



## Pavement Structure

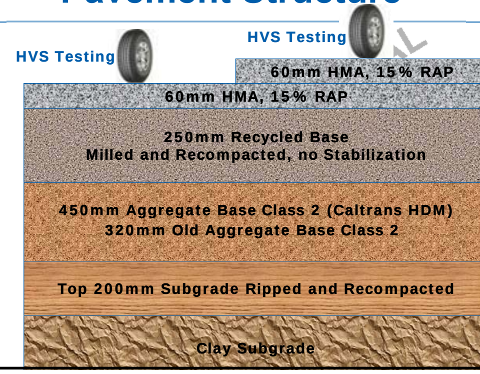


## Instrumentation

- Strain Gauges
- Pressure Cells
- Multi-Depth Deflectometers
- Thermocouples

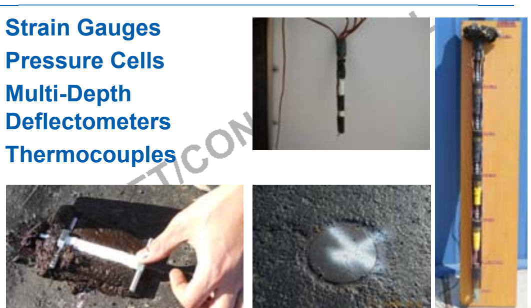





## Instrumentation

- Thick Section
  - 8 Strain Gauges (two malfunctioned, 1 const, 1 testing)
  - 4 Pressure Cells
  - 1 MDD hole with three depths
  - 12 Thermocouples
- Thin Section
  - 6 Strain Gauges (two malfunctioned in testing)
  - 1 Pressure Cell
  - 1 MDD hole with four depths
  - 12 Thermocouples

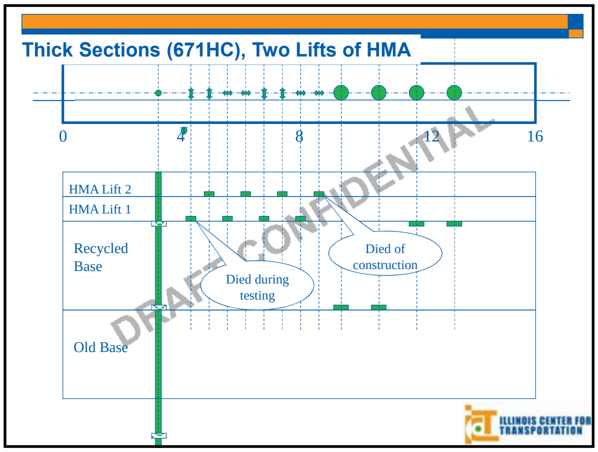
Thick Sections (671HC), Two Lifts of HMA
0
4
8
12
16
HMA Lift 2
HMA Lift 1
Recycled Base
Old Base
Died during testing
Died of construction
DRAFT/CONFIDENTIAL


Thick Section
On Top of the Recycled Aggregate Base

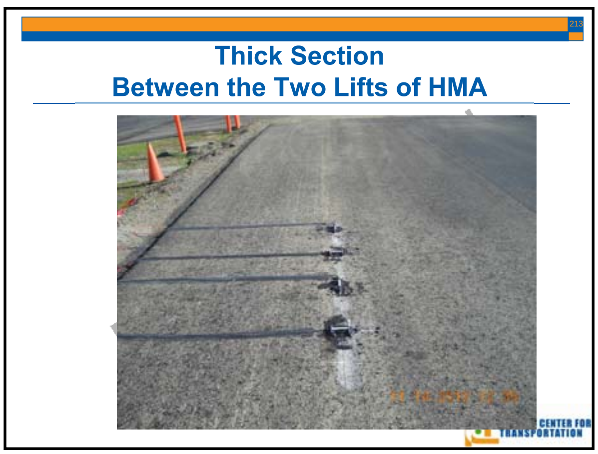
Thick Section
Between the Two Lifts of HMA

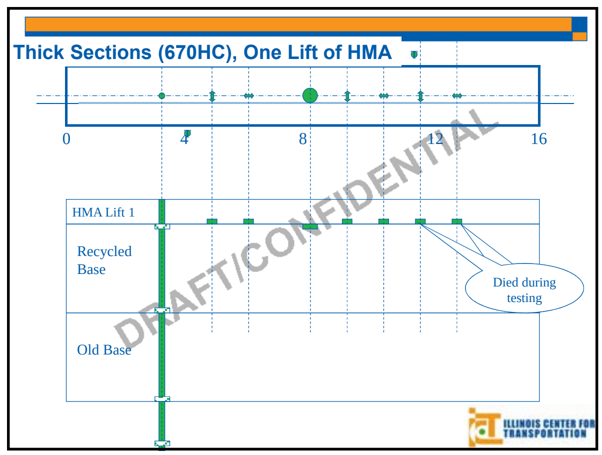
Thick Sections (670HC), One Lift of HMA
0
4
8
12
16
HMA Lift 1
Recycled Base
Old Base
Died during testing
DRAFT/CONFIDENTIAL


Thin Section
On Top of the Recycled Aggregate Base

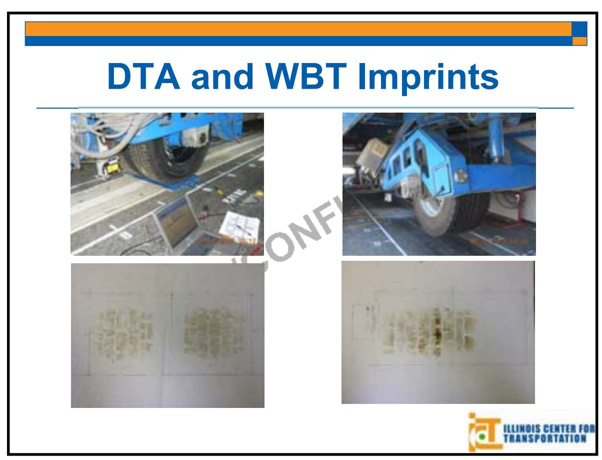
DTA and WBT Imprints

## HVS Testing Program – 1/3

- Full Factorial
  - HMA Thickness (2.4 and 4.7 in)
  - Pavement Temperature (69, 95, 122F)
  - Tire Pressure (80,100,110,125 psi for both, 60/110, 80/110 psi for dual)
  - Half Axle Load (6, 8, 10, 14, 18 kips)
- Partial Factorial
  - Lateral Offset (0, 7, 12 in)
- Spot Check (by repetition) in the end





## HVS Testing Program – 2/3

- Testing Sequence
  - Perform permutations for half axle loads less than 18 kips
    - Wheel type (WBT, DTA)
    - Temperature
    - Tire pressure
    - Load
  - Then repeat with half axle load at 18 kips
    - To prevent excessive damage at 18 kips
  - Spot check (repeat selected combinations)
    - Wheel type
    - Temperature
    - Tire pressure







## HVS Testing Program 3/3

- 174 combinations in total
- Each combination:
  - 100 repetitions
  - Constant speed of 8 km/h
  - Channelized (no wander)
- Thick Section
  - 3/6/2013~4/15/2013
  - 22,100 repetitions total
- Thin Section
  - 4/26/2013~5/20/2013
  - 20,300 repetitions total







## Data Collection

- Record every repetition:

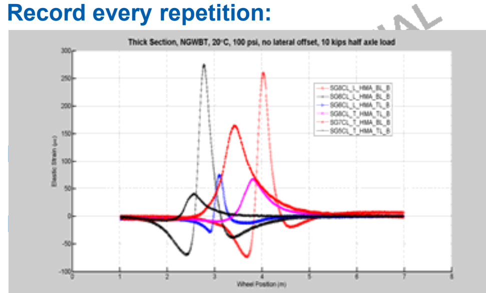






## After HVS Testing – Thin Section




## Surface Rut Contour – Thin Section

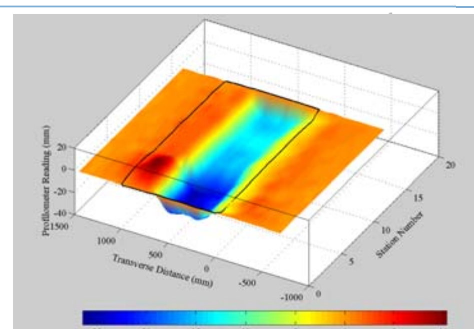

## After HVS Testing – Thick Section

## Surface Rut Contour – Thick Section

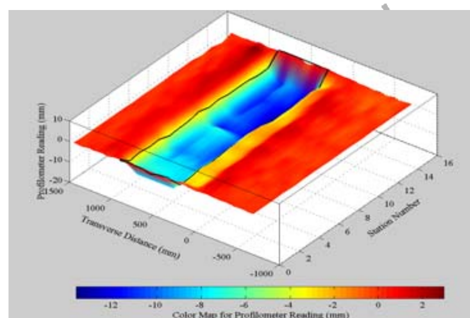


## Example of Preliminary Results – Thin Section, Horizontal Strain at Bottom of the HMA

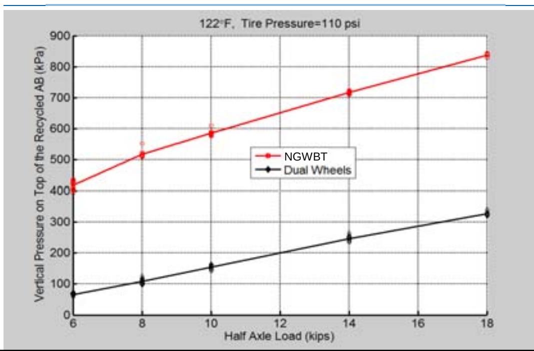


## Example of Preliminary Results – Thin Section, Longitudinal Strain at Bottom of HMA (First Lift)

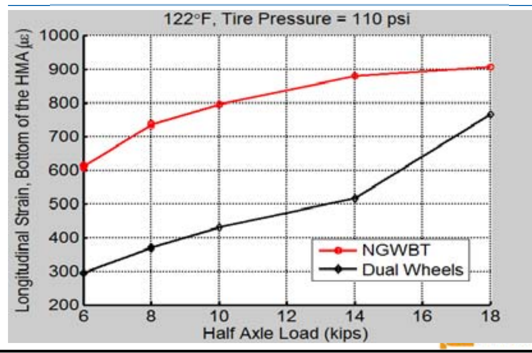


## Definition of Lateral Offset

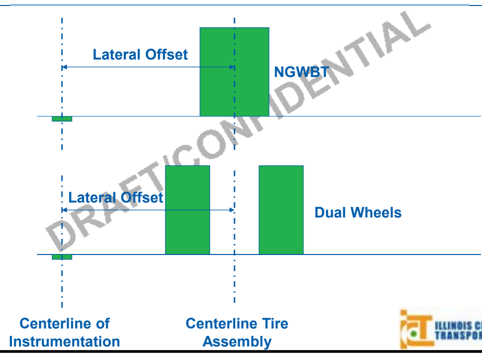


## Preliminary Results – Strain in Thick Section, Effect of Lateral Offset

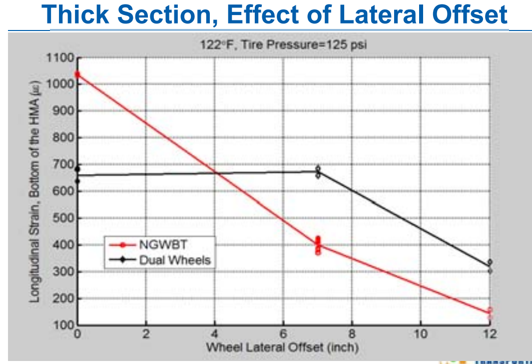

## LCA - Basic Approach

- Select scenarios for pavement network based on:
  - Traffic level
  - Pavement Structure
- For each scenario perform LCA
  - Using existing inventories
- Additional sensitivity analyses on:
  - Market penetration rates, types, traffic levels, congestion levels, etc.
- Deliverables:
  - Framework for LCA
  - Provide guidance for decision makers on impact of NGWBT
  - Suggest particular scenarios where impact is greater



ILLINOIS CENTER FOR TRANSPORTATION

## Framework for LCA

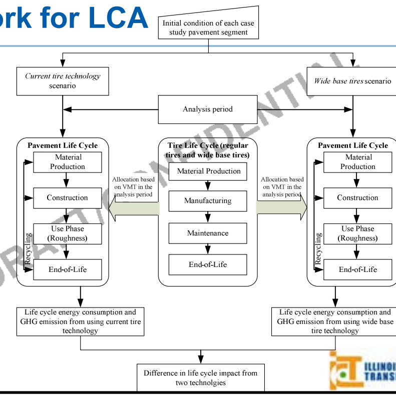




ILLINOIS CENTER FOR TRANSPORTATION

231

## Remarks

- Significant difference in pavement responses between Dual and NGWBT were observed.
- Testing caused rutting in the pavement, which did not affect the relative comparison.
- Effect of wheel lateral offset needs to be considered when making comparisons.
- LCA framework established, will need some inputs to the model.



ILLINOIS CENTER FOR TRANSPORTATION

232

## Future Plans

- Complete APT test matrix
- Data collection for life-cycle inventory
- LCA case studies



ILLINOIS CENTER FOR TRANSPORTATION

## COMMENTS!



ILLINOIS CENTER FOR TRANSPORTATION

## Instrumentation and Testing: Ohio

OHIO UNIVERSITY



ILLINOIS CENTER FOR TRANSPORTATION

## Outline

- Project description
- Typical section
- Instrumentation
- Material sampling
- Controlled loading test



OHIO UNIVERSITY | ILLINOIS CENTER FOR TRANSPORTATION

## Project Description

- Located in Delaware, OH (US-23)
- Optimization of AC thickness in perpetual pavements
- Three heavily instrumented pavement sections (AC thickness: 13 and 15 in)
- Truck load test: WBT and DTA; single and tandem axle



OHIO UNIVERSITY | ILLINOIS CENTER FOR TRANSPORTATION

## Typical Section

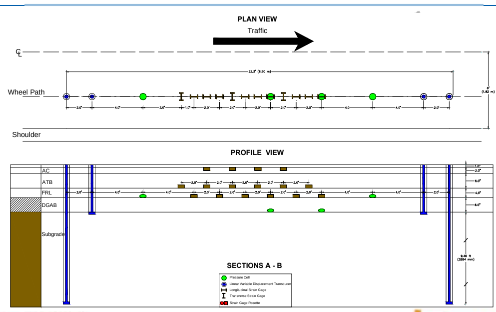


OHIO UNIVERSITY | ILLINOIS CENTER FOR TRANSPORTATION

## Instrumentation

- Deep and shallow LVDTs
- Pressure cells at the bottom of AC and base
- Thermocouples
- Strain gauges in longitudinal and transverse directions at various depths
- Rosettes strain gauges



OHIO UNIVERSITY | ILLINOIS CENTER FOR TRANSPORTATION

## Pressure Cells

Pressure cells on top of subgrade

Pressure cells on top of DGAB

OHIO UNIVERSITY | ILLINOIS CENTER FOR TRANSPORTATION

## Strain Gauges

OHIO UNIVERSITY | ILLINOIS CENTER FOR TRANSPORTATION

## Strain Gauges Rosettes



## Material sampling

Loose mix from each material (layer)



## Material sampling

Compacted samples from each material (layer)





## Controlled Truck Loading Test

| Tire load (kip) | Speed (mph) | Tire pressure (psi) | Tire configuration | Axle Configuration |
|---|---|---|---|---|
| 10, 14 | 5, 30, and 55 | 80, 110, 125 | WBT-445 & DTA-275 | Single & Tandem |

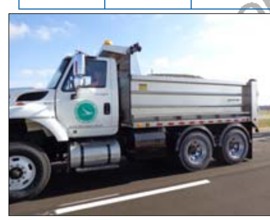

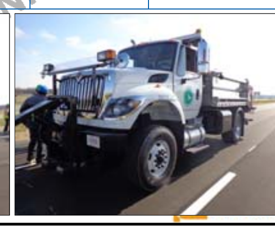



## Controlled Truck Loading Test




## Controlled Truck Loading Test

## COMMENTS!





## Future Plans Discussion
**3:30-3:45pm**

5/30/2013







## Future Plans

- Contact stresses
  - Complete detailed contact stress analysis of DTA and WBT magnitude and distribution
  - Prediction of contact stresses using FEM
- Modeling
  - Complete thin and thick pavement cases with various combinations of axle loads and tire inflation pressures
  - Provide a analysis considering the effect of tire type; material property; loading characteristics; and pavement structure







## Future Plans

- Laboratory testing:
  - Compact SGC specimens that simulate field-compacted samples (air void validation)
  - Complete laboratory test matrix for materials in all testing sites
- Complete APT and field-instrumented data collection and analysis
- Finalize the instrumentation response database
- Preliminary LCA scenarios
- Marketing and publications





## COMMENTS!





## Technical Committee Discussion
**3:45-4:15pm**

5/30/2013

## COMMENTS!





## Final Remarks

**4:15-4:45pm**



5/30/2013